An Orphaned Baltic Terrane in the Greenland Caledonides: A Sm-Nd and Detrital Zircon Study of a High-Pressure/Ultrahigh-Pressure Complex in Liverpool Land

H. K. Brueckner,[1,2,*] *L. G. Medaris Jr.,*[3] *E. A. Belousova,*[4] *S. M. Johnston,*[5] *W. L. Griffin,*[4] *E. H. Hartz,*[6] *S. Hemming,*[1] *E. Ghent,*[7] *and R. Bubbico*[2]

1. Lamont-Doherty Earth Observatory of Columbia University, Palisades, New York 10964, USA; 2. Queens College and the Graduate Center, City University of New York, Queens College, Flushing, New York 11367, USA; 3. Department of Geoscience, University of Wisconsin, Madison, Wisconsin 53706, USA; 4. Australian Research Council (ARC) Key Centre for Geochemical Evolution and Metallogeny of Continents and Department of Earth and Planetary Sciences, ARC Centre of Excellence for Core to Crust Fluid Systems, Macquarie University, New South Wales 2109, Australia; 5. Physics Department, California Polytechnic State University, San Luis Obispo, California 93407, USA; 6. Center for Earth Evolution and Dynamics (CEED), Postbox 1028 Blindern, N-0315 Oslo, Norway; 7. Department of Geoscience, University of Calgary, Calgary, Alberta T2N 1N4, Canada

ABSTRACT

Liverpool Land, at the southern tip of the Greenland Caledonides, exposes a composite metamorphic terrane: the midcrustal granulite-facies Jaettedal Complex tectonically juxtaposed against the eclogite-facies, peridotite-bearing Tvaerdal Complex. The Jaettedal Complex is a Laurentian terrane, whereas the Tvaerdal Complex was proposed by earlier investigators to be a Baltic terrane. *PT* estimates (880°–920°C at 35–40 kbar) and Sm-Nd mineral isochrons from Tvaerdal eclogites indicate that recrystallization occurred under ultrahigh-pressure (UHP) metamorphic conditions ≈400 m.yr. ago, the same time and under similar conditions as the Western Gneiss Complex of the Norwegian Caledonides. Detrital zircons from the Tvaerdal Complex, analyzed for U-Pb, Lu-Hf, and trace elements by laser ablation inductively coupled plasma mass spectrometry, give concordant Mesoproterozoic ages but not the Archean and ≈1.8 Ga Proterozoic ages characteristic of Laurentian terranes. Most remaining concordant U-Pb ages are 411–375 Ma (i.e., Scandian), which contrast with older (≈460–410 Ma) zircon ages from the Jaettedal Complex as well as other Laurentian terranes. Both the Precambrian and the Scandian age sets confirm the Tvaerdal Complex as an orphaned Baltic terrane. The Jaettedal Complex underwent a lengthy Caledonian history as part of a continental arc system during the closure of Iapetus, whereas the Tvaerdal Complex was a fragment of the approaching Baltic passive margin. UHP metamorphism occurred when this margin subducted into the mantle beneath Laurentia. We propose that the Tvaerdal Complex separated from Baltica and rose through the hot mantle wedge to the base of the overriding Laurentian crust by diapirism, a process that may explain its abundant anatectic granitoid intrusions.

Online enhancements: appendixes, supplemental tables and figures.

Introduction

Liverpool Land, at the southern end of the Greenland Caledonides (fig. 1), exposes high-grade metamorphic rocks, including eclogites and garnet-bearing harzburgite/dunite/pyroxenite lenses, intruded by numerous granitoid bodies (fig. 2*A*) on all size scales. A granitic igneous suite, the Hurry Inlet Plutonic Terrane, occurs tectonically above and to the north of the metamorphic rocks. The presence of eclogites within the metamorphic terrane led Augland et al. (2010) to call it the Liverpool Land Eclogite Terrane. However, Johnston et al. (2010) revealed that eclogites (and peridotites) are restricted to a portion of the metamorphic terrane, which they called the

Manuscript received October 26, 2015; accepted May 2, 2016; electronically published August 18, 2016.

* Author for correspondence; e-mail: hannes@ldeo.columbia.edu.

[The Journal of Geology, 2016, volume 124, p. 000–000] © 2016 by The University of Chicago. All rights reserved. 0022-1376/2016/12405-00XX$15.00. DOI: 10.1086/687552

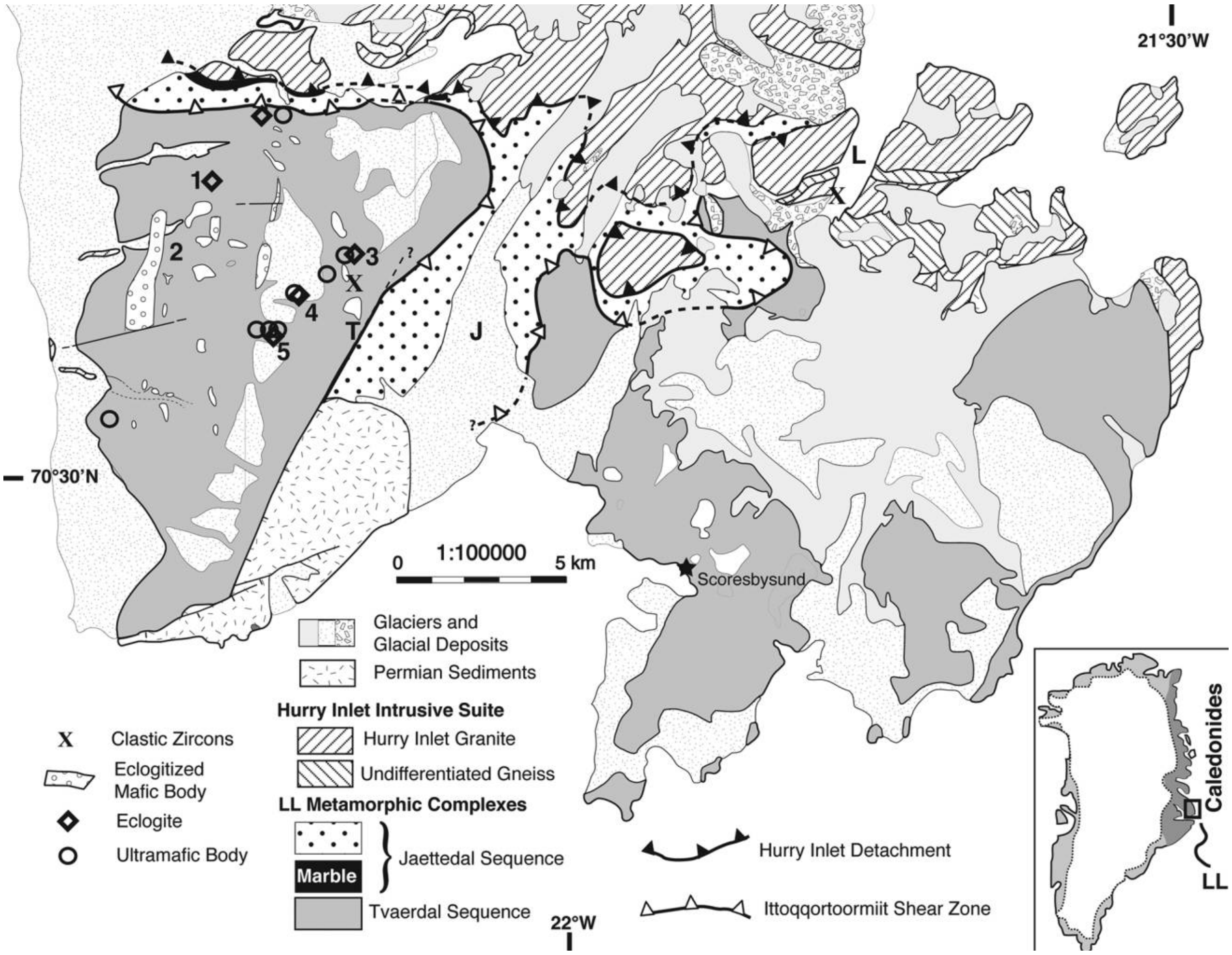

Figure 1. Simplified geologic map of the Liverpool Land (LL) high-pressure terrane showing the distribution of the Tvaerdal, Jaettedal, and Hurry Inlet Plutonic Complexes. Numbers refer to localities of eclogites analyzed in this study (see also table 1). Detrital zircons were collected at sites marked with an X. Simplified from Johnston et al. 2010. J = Jaettedal; L = Lillefjord; T = Tvaerdal. A color version of this figure is available online.

Tvaerdal Complex (fig. 1). The rest of the metamorphic rocks of Liverpool Land, which they named the Jaettedal Complex (Johnston et al. 2010, 2015), comprise a granulite-facies terrane that had an independent history until the two terranes were juxtaposed at roughly 400 Ma. The existence of two metamorphic terranes and the nature of a tectonic boundary that separates them are still being debated, but in the interests of consistency with our earlier publication, we continue to divide the metamorphic rocks of Liverpool Land into the eclogite-facies Tvaerdal Complex and the granulite-facies Jaettedal Complex. Johnston et al. (2015) present U-Pb zircon ages and pressure-temperature information that demonstrated that the Jaettedal Complex is a Laurentian terrane that underwent a prolonged Paleozoic evolution along the eastern margin of Laurentia during the closure of Iapetus. Several recent studies of the eclogites and host gneisses of the Tvaerdal Complex (Augland et al. 2010, 2011; Johnston et al. 2010; Corfu and Hartz 2011) revealed that the Tvaerdal Complex is largely composed of Middle and Late Proterozoic igneous rocks that recrystallized under high-pressure (HP) and possibly ultrahigh-pressure (UHP) conditions at roughly 400 Ma, coinciding with the Scandian orogeny of the Scandinavian Caledonides on the east side of the North Atlantic. The similarities of the Tvaerdal Complex with the Western Gneiss Complex (WGC) of the Norwegian Caledonides led most of the authors of these studies to propose that the Tvaerdal Complex was originally a fragment of Baltica and perhaps even contiguous with the WGC (a contrary view is presented at the end of Corfu and Hartz 2011).

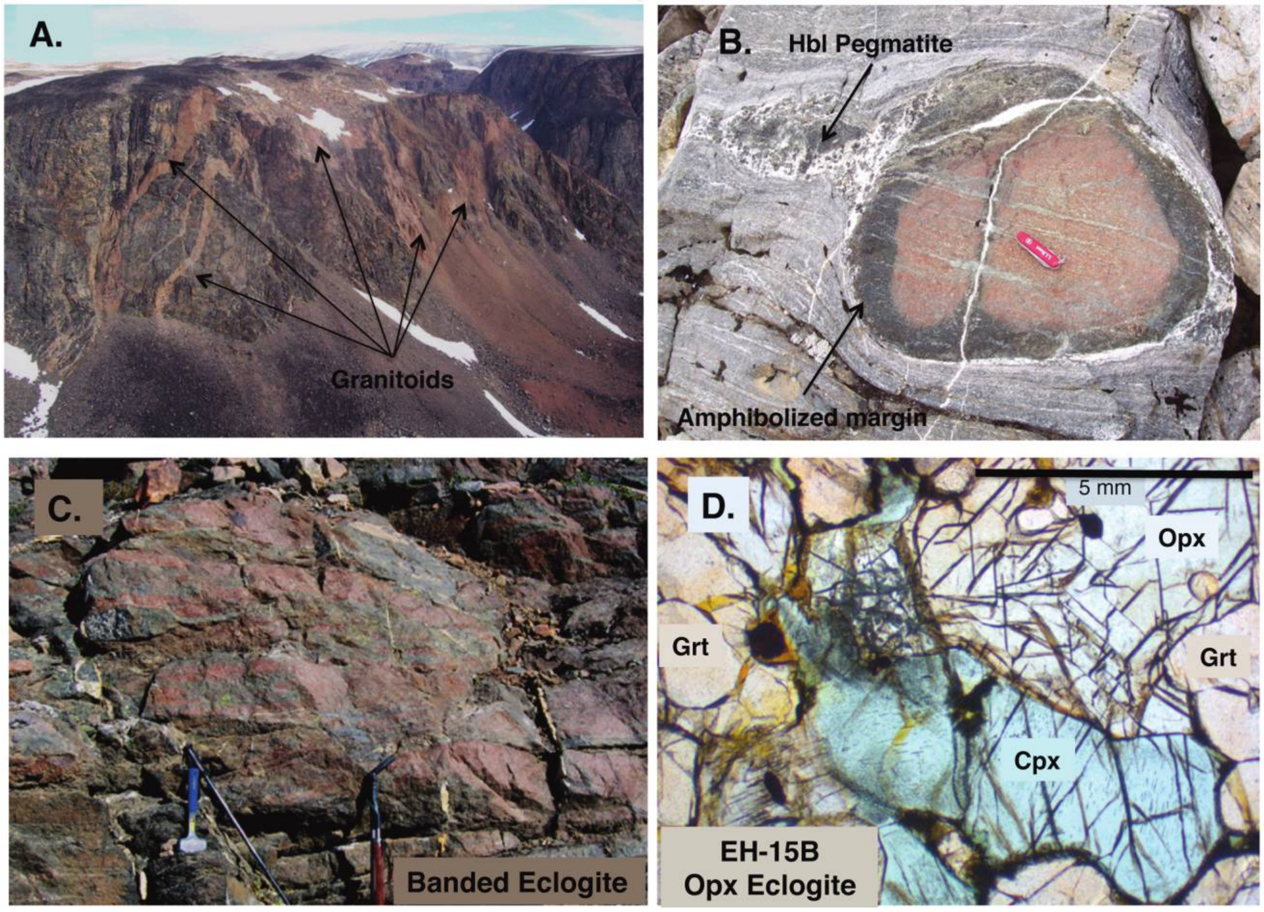

Figure 2. *A*, North wall of Tvaerdal showing abundant granitoids, characteristic of the Tvaerdal Complex. *B*, Eclogite boudin showing amphibolitized margins and associated hornblend-rich pegmatite. *C*, Field image of a banded eclogite with alternating clinopyroxene-rich, garnet-rich, and orthopyroxene-rich layers. *D*, Thin section of orthopyroxene-bearing eclogite EH-15B.

These conclusions raise a dilemma. If the Scandian orogeny involved the subduction of Baltica (Scandinavia) beneath Laurentia (Greenland), as is generally believed (for recent reviews, see Andersen et al. 1991; Brueckner and Van Roermund 2004; Hacker et al. 2010; Gee et al. 2012; Gasser 2014), how did the Tvaerdal Complex become part of the Greenland Caledonides (i.e., the upper plate) instead of returning along with the WGC as part of the Scandinavian Caledonides (the lower plate). Alternatively, perhaps it was always part of Laurentia (Hartz et al. 2005, 2007), as has been demonstrated for the Northeast Greenland Eclogite Terrane in northern Greenland (Gilotti and McClelland 2007). If so, what mechanism caused the Tvaerdal Complex to undergo eclogite-facies metamorphism, and how did it pick up mantle peridotite bodies?

We present new information on the Tvaerdal Complex and its eclogites as well as from the structurally higher Hurry Inlet Plutonic Complex (HIPC). Eclogite minerals were analyzed for major and trace element concentrations and dated by Sm-Nd mineral isochron and Ar-Ar biotite methods. The results confirm a Scandian age for the evolution of the eclogites and add new information on their pressure-temperature-time (*PTt*) evolution. We also collected detrital zircons, rutiles, and titanites from modern stream and beach sediments, analyzed them for trace elements and Hf isotopes, and dated them by U-Pb via laser ablation inductively coupled plasma mass spectrometry (LA-ICP-MS). The analytical techniques for all studies are available in appendix 1 (apps. 1–4 are available online). The data from HIPC detrital zircons confirm earlier proposals of a magmatic history for the HIPC between 470 and 410 Ma and are reviewed briefly in the supplemental material. The detrital zircons from the Tvaerdal Complex reveal new information. Zircons with pre-Scandian U-Pb ages define Proterozoic age patterns that support, but do not prove, that the Tvaerdal

Complex originated as part of Baltica. However, zircons with Scandian ages document a relatively short HP/UHP history for the Tvaerdal Complex (411–375 Ma) that contrasts with the older and more prolonged events recorded in the adjacent Jaettedal Complex (460–412 Ma; Johnston et al. 2015), thereby providing a more compelling argument for a Baltic origin for the Tvaerdal Complex.

Regional Setting

The Greenland Caledonides. The tectonic relationships of the Greenland Caledonides to Liverpool Land are well reviewed in Augland et al. (2010, 2011), Johnston et al. (2010, 2015), Johnston and Kylander-Clark (2013), and Corfu and Hartz (2011). The mountain system is composed of several west-vergent nappes or thrusts, mirror images in many ways to the east-directed thrusts of the Scandinavian Caledonides. The three allochthons are, from bottom to top, the Niggli Spids, the Hagar Bjerg, and the Franz Joseph (Henriksen 2003; Higgins et al. 2004). The foreland shield and the two lower thrust sheets consist of Archean and Paleoproterozoic gneisses (Kalsbeek 1995; Thrane 2002) overlain by the latest Paleoproterozoic Krummedal sequence, while the Franz Joseph allochthon consists primarily of a thick succession of Neoproterozoic to Ordovician sedimentary rocks known as the Eleonore Bay Supergroup. Recent dating of the basal Niggli Spids thrust sheet reveals an extensive Archean history with magmatic events at ≈3.6 and ≈3.0 Ga and metamorphism and intrusion at ≈2.7 Ga (Johnston and Kylander-Clark 2013). The generally accepted, seemingly simple west-directed thrust history of the allochthons during the Caledonian orogeny has been modified by the recent discovery of faults that are syn- to late-orogenic extensional detachments with both top-to-the-east and orogen-parallel displacement (Hartz et al. 2001; Jones and Strachan 2000; Gilotti and Elvevold 2002; White and Hodges 2002; Gilotti and McClelland 2007). About 100 km of postorogenic basin deposits separates these allochthons from the Liverpool Land crystalline complexes. Nevertheless, detrital zircon spectra similar to those presented here as well as similar magmatic and metamorphic histories (e.g., Johnston et al. 2010, 2015; Augland et al. 2011) suggest that correlations with these terranes are possible, as discussed further below.

Liverpool Land Crystalline Rocks. Cheeney (1985) divided the crystalline rocks of Liverpool Land into a largely magmatic and a largely metamorphic complex. The magmatic complex to the north is the HIPC, which rests on top of the metamorphic southern complex (fig. 1). The two units are separated by the thick, north-dipping Gubbedalen shear zone.

HIPC. Earlier studies indicate that the HIPC formed in two episodes of plutonism: a granite to granodiorite suite between 446 and 430 Ma, followed by a monzonitic suite between 426 and 424 Ma (Krank 1935; Hansen and Steiger 1971; Coe 1975; Hansen and Friderichsen 1987; Henriksen 2003; Corfu and Hartz 2011; Augland et al. 2012). The thermal history of the HIPC appears to have ended roughly by 415 Ma. Geochemical studies from the HIPC suggest that the plutons are part of the alkali-calcic to calc-alkaline continental arc that developed on the eastern Laurentian margin during the closure of Iapetus (Augland et al. 2012).

We obtained U-Pb ages and Hf isotope data by in situ laser ablation techniques from detrital zircons collected along the shore of Lillefjord, at the southern margin of this plutonic suite, and they broadly confirm the conclusions of the earlier studies. The data do not add significant geochronological information to these earlier studies, but the U-Pb age and Hf isotope pattern of the HIPC contrasts sharply with the pattern defined by zircons from the Tvaerdal Complex, as discussed and illustrated later in this article. Therefore, we have placed the data, some figures, and a short discussion in appendix 2.

The Metamorphic Complexes. The metamorphic complexes underlying the HIPC comprise a relatively small area (fig. 1) but are covered by fjords to the south and west, and it might be considerably larger. As noted above, Johnston et al. (2010) subdivided it into a tectonically lower orthogneiss sequence (the Tvaerdal Complex) separated by the Ittoqqortoormiit shear zone from a tectonically higher, more heterogeneous unit containing orthogneiss but also granulites, pelitic schists, calc-silicate rocks, and marbles (the Jaettedal Complex). A further, very important distinction is that the Tvaerdal Complex contains lenses of eclogite and peridotite, as well as clinopyroxene in the gneisses, indicating metamorphism under high and possibly ultrahigh eclogite-facies pressures as well as exposure of the mantle. The Jaettedal Complex lacks eclogites and peridotites and reached granulite-facies, rather than eclogite-facies, conditions (Johnston et al. 2010, 2015). Despite these differences, both units have an overall homogenous reddish color when viewed from a distance caused by abundant K-feldspar-rich synkinematic and postkinematic granitoid sills, dikes, and other small intrusions (fig. 2*A*).

The north-dipping, low-angle Gubbedalen shear zone separates the metamorphic complexes from the structurally higher HIPC. It contains pervasive top-N shear-sense indicators and is therefore interpreted as a low-angle, normal-sense detachment resulting from the southward displacement and exhumation of the metamorphic complexes relative to the overlying HIPC (Augland et al. 2010; Johnston et al. 2010). The base of the metamorphic complexes is not exposed, so we cannot determine whether this exhumation occurred by orogen-parallel extension or by southward extrusion.

Johnston et al. (2010) proposed that the structurally lower contact between the Jaettedal and Tvaerdal Complexes (fig. 1) is another tectonic boundary, which they called the Ittoqqortoormiit shear zone. Shear-sense indicators at the highest levels of the Tvaerdal Complex and along its contact with the overlying Jaettedal Complex yield top-south, top-southwest, and symmetrical motions that predate the top-north displacement along the Gubbedalen shear zone. This relationship suggests that the Tvaerdal and Jaettedal Complexes were juxtaposed in the lower to middle crust before their juxtaposition with the HIPC along the Gubbedalen shear zone. This earlier event presumably occurred as the Liverpool Land eclogite terrane was exhumed from the upper mantle and came into contact with the Laurentian lower crust. The subsequent shared intrusive history of the two complexes occurred during further exhumation from beneath the Hurry Inlet Arc Terrane along the Gubbedalen shear zone.

Eclogites of the Tvaerdal Complex

Cheeney (1985) was the first to publish the presence of eclogites within the Tvaerdal Complex. They are further described in several recent publications, dissertations, and abstracts (Hartz et al. 2005; Augland 2007; Bowman 2008; Buchanan 2008; Augland et al. 2010, 2011; Johnston et al. 2010; Corfu and Hartz 2011). Eclogites occur in and to the west of the Tvaerdal valley (T in fig. 1) as meter-scale boudins (fig. 2*B*) and boudin trains and as portions of decameter- to kilometer-sized mafic lenses, locally intensely folded. A detailed transect of one large mafic body >800 m perpendicular to its strike revealed it to be composed largely of well-preserved to partially retrogressed (i.e., pyroxene-garnet-amphibole symplectites) eclogite. There are also minor (<10%) intercalated layers of felsic gray gneiss composed of quartz + plagioclase + garnet + biotite ± clinopyroxene. We did not observe original igneous minerals or textures with the possible exception of banding (fig. 2*C*). The smaller mafic boudins also display fresh eclogite-facies minerals that are partially to completely retrogressed to amphibolite-facies assemblages, particularly along their margins (fig. 2*B*). Coarse hornblende − plagioclase ± garnet (relict?) pegmatites that occur locally in boudin necks (fig. 2*B*) or as isolated boudins within adjacent felsic orthogenisses suggest that H_2O-expedited anatectic melting of the gneisses during decompression caused disaggregation and partial assimilation of the eclogites or their hydrated equivalents.

The most common eclogite (table 1) is massive and medium grained and contains omphacite + garnet ± quartz, while coarser-grained, massive orthopyroxene + clinopyroxene + garnet ± biotite eclogite (fig. 2*D*) is less common, as are banded eclogites composed of alternating garnet-rich and clinopyroxene-rich layers or alternating orthopyroxene-rich and orthopyroxene-poor layers (fig. 2*C*). Zircon, rutile (locally altered to ilmenite), and apatite are common accessory minerals, occurring within garnet and clinopyroxene and within the matrix. Quartz inclusions are relatively common, but only one of the many examined samples displays radial cracks that might suggest the former presence of coesite. Garnet commonly contains exsolved needles of rutile. Layered eclogites display tight to isoclinal folds that are geometrically similar to folds in the enclosing gneisses, suggesting that the eclogites, or their protoliths, were deformed along with their host gneisses in the crust.

Eclogite Chemistry. Table 1 lists eclogite sample localities, geographical coordinates, mineral modes, and core and rim mineral compositions determined by electron microprobe (EMP) analyses. Additional eclogite mineral point analyses are in table S1 (tables S1–S4 are available online) as well as in Augland et al. (2010) and Buchanan (2008). Samples studied in detail here include bimineralic (garnet + clinopyroxene) eclogites EH-81, initially described by Hartz et al. (2005), and EH-25, which is part of a larger orthopyroxene eclogite body in Tvaerdal described and dated by U-Pb in Corfu and Hartz (2011); orthopyroxene eclogite EH-15B in Rendelv (fig. 2*D*); and biotite eclogite HKB-6B from west of Tvaerdal (see locations in fig. 1). The average garnet composition in orthopyroxene eclogite EH-15B is ($Py_{47.3}Alm_{41.2}Grs_{10.4}Sp_{1.0}$), whereas garnet in bimineralic eclogites EH-25 and EH-81 is more pyrope rich ($Py_{63}Alm_{28}Grs_9Sps_1$ and $Py_{51}Alm_{39}Grs_9Sps_1$, respectively). Clinopyroxene in eclogite EH-25 is omphacite ($Ac_2NaCr_3Jd_{31}CaTs_2Di_{47}Hd_{10}En_7Fs_1$), but in EH-15B and EH-81 clinopyroxene is sodic augite ($Ac_5Jd_6CaTs_2Di_{68}Hd_{11}En_7Fs_1$ and $Ac_7Jd_{16}CaTs_2Di_{57}Hd_{10}En_7Fs_1$, respectively), probably due to relatively low whole-rock sodium contents. Orthopyroxene in EH-15B is enstatite (average Mg# of 75.9). Amphibole compositions vary from pargasite in eclogite to actinolite

Table 1. Eclogite Sample Localities, Mineral Abundances, and Core and Rim Mineral Compositions Used for *PT* Calculations

Sample no.:	EH-81 (70°34.033N, 022°18.350W, locality 1)				EH-25 (70°33.842N, 022°10.547W, locality 3)				EH-15B (70°33.158N, 022°20.520W, locality 2)					
Mineral %:	cpx 35, grt 60, amph 5, rut tr.				cpx 15, grt 85, rut and ap tr.				opx 15, cpx 20, grt 60, amph 5, rut 1 banded, 2-cm grt, 5-cm opx					
	AMNH cpx core	AMNH cpx rim	AMNH grt core	AMNH grt rim	AMNH cpx core	AMNH cpx rim	AMNH grt core	AMNH grt rim	AMNH cpx core	AMNH cpx rim	AMNH grt core	AMNH grt rim	McQ LoAlopx	McQ HiAlopx
SiO_2	54.68	54.72	40.43	40.21	55.20	55.10	41.41	40.97	55.08	54.82	38.60	39.80	55.89	54.70
TiO_2	.12	.13	.06	.04	.21	.20	.04	.05	.05	.08	.06	.05	.01	.05
Al_2O_3	4.33	4.66	22.49	22.36	8.09	8.36	22.74	22.12	2.09	2.37	21.35	21.77	.59	2.17
Cr_2O_3	.06	.06	.06	.07	1.14	1.12	.80	.77	.05	.00	.05	.04	.00	.00
FeO	6.11	6.18	19.50	20.01	3.51	3.48	14.09	15.23	5.83	5.97	20.00	20.10	15.82	15.80
MnO	.08	.09	.52	.56	.06	.08	.48	.59	.06	.05	.54	.53	.13	.16
MgO	13.09	12.87	14.14	13.57	11.40	11.50	18.01	16.39	15.17	14.96	12.50	12.70	28.33	27.95
CaO	18.00	17.77	3.64	3.76	15.60	15.60	3.39	3.66	21.14	20.83	4.31	4.43	.29	.41
Na_2O	3.30	3.41	.03	.03	4.86	4.79	.03	.03	1.64	1.69	.02	.02	.04	.01
NiO	.10	.10	.01	.01	.05	.04	.01	.01	.06	.05	.01	.01	.06	.04
Total	99.86	99.98	100.88	100.61	100.12	100.27	101.00	99.81	101.18	100.82	97.44	99.45	101.16	101.29
		Avg.		Avg.		Avg.		Avg.		Avg.		Avg.		
	Acm	.069	%Alm	39.1	Acm	.007	%Alm	27.7	Acm	.051	%Alm	27.7		
	NaCr	.002	%Sps	1.06	NaCr	.032	%Sps	.95	NaCr	.001	%Sps	.95		
	Jd	.156	%Prp	50.5	Jd	.296	%Prp	62.8	Jd	.062	%Prp	62.8		
	CaTs	.017	%Grs	9.37	CaTs	.024	%Grs	8.52	CaTs	.023	%Grs	8.52		
	Jh	.003			Jh	.002			Jh	.002				
	Di	.573	Mg#	56.4	Di	.490	Mg#	69.4	Di	.678	Mg#	69.4		
	Hd	.098			Hd	.079			Hd	.110				
	En	.074			En	.060			En	.065				
	Fs	.013			Fs	.010			Fs	.011				
	Sum	1.003			Sum	1.000			Sum	1.002				
	X Jd	.155			X Jd	.296			X Jd	.062				
	X Di	.571			X Di	.490			X Di	.676				

Note. *PT* of EH-15B was calculated from average clinopyroxene and garnet (table S2) and low and high aluminum in orthopyroxene. For HKB-6B (70°33.000N, 22°12.720W, locality 4; cpx 51, grt 41, sp 6, bi 6, amph 2), minerals were not analyzed for major elements. HKB-7 (70°35.907N, 22°13.439W, locality 5; retrograded symplectite-biotite-amphibole eclogite) was analyzed for Ar-Ar dating only. AMNH = electron microprobe (EMP) analysis, American Museum of Natural History, New York (data from table S2); McQ = EMP analysis, Macquarie University, Sydney (data from table S2).

in retrograded domains, reflecting recrystallization over a range of pressure and temperature, decreasing from UHP to retrograde conditions.

Table S1 also lists scans of minerals from eclogites EH-15B, EH-25, and EH-81. Figure S1 (figs. S1, S2 are available online) displays EMP backscatter electron images and X-ray maps for selected major elements in orthopyroxene eclogite EH-15B and biotite eclogite HKB-6B. The concentrations of most major and trace elements do not appear to vary significantly from core to rim for most mineral grains except for sharp increases in Al toward the rims of orthopyroxene and, to a lesser extent, clinopyroxene in the orthopyroxene eclogite. The EMP scans across selected orthopyroxenes (fig. 3) in EH-15B show this increase in aluminum content quite dramatically (fig. 3*A*, 3*B*). Other point analyses show Al_2O_3 to be as low as 0.59% in some grains and as high as 2.17% in others (table 1). Most garnets show flat concentration patterns for most elements throughout most of the grain, with some slight variations toward the rim. Bimineralic eclogite EH-81, for example, shows a small decrease in MgO and an increase in FeO very close to the rim (fig. 3*C*), whereas the smaller grains in eclogite EH-25 (fig. 3*D*) shows similar changes in the outer third of the garnet grain. Clinopyroxenes show a decrease in CaO and MgO accompanied by an increase in Al_2O_3 near the rims in EH-81 (fig. 3*C*) and, to a lesser extent, EH-25 (fig. 3*D*). The core-to-rim compositional patterns in eclogite do not exhibit those expected from prograde metamorphism, and we suggest that recrystallization at high temperatures homogenized the phases and erased any prograde record in the samples analyzed.

Pressure-Temperature Calculations. Pressure and temperature conditions for the Tvaerdal eclogite suite are best constrained by orthopyroxene eclogite EH-15B because the presence of orthopyroxene allows pressure to be estimated from the Al-in-Opx geobarometer (Nickel and Green 1985; Brey and Köhler 1990; Brey et al. 2008), and temperature can be estimated by both Grt-Opx Fe-Mg exchange geothermometry (Harley 1984) and 2-pyroxene geothermometry (Brey and Köhler 1990; Taylor 1998). Application of these geothermobarometers to the core compositions of orthopyroxene (low Al), clinopyroxene, and garnet yield UHP conditions with a peak pressure of ~37 kbar and temperature of ~900°C (fig. 4). In contrast, a high-Al orthopyroxene yields a pressure of ~16 kbar and temperature of ~800°C (fig. 4), reflecting a stage in the nearly isothermal decompression of the eclogite suite when intergrain elemental exchange effectively ceased.

Another approach is to calculate a model pressure and temperature for orthopyroxene eclogite by application of Theriak/Domino software (de Capitani and Petrakis 2010), which uses the whole-rock composition for EH-15B and calculated mineral compositional isopleths to produce an intersection in *PT* space. Calculated isopleths for Mg-tschermak in orthopyroxene (mole fraction = 0.01) and almandine in garnet (mole fraction = 0.45) intersect at 960°C at 35 kbar, which is in good agreement with the results from conventional geothermobarometry.

Additional temperature estimates for orthopyroxene-free eclogite can be obtained by application of the Grt-Cpx Fe-Mg exchange geothermometer, and five calibrations of this geothermometer (Powell 1985; Ai 1994; Ganguly et al. 1996; Ravna 2000; Nakamura 2009) have been applied to two eclogite samples investigated here, EH-25 and EH-81, and an eclogite analyzed by Augland et al. (2010). However, temperatures derived from this method are sensitive to the Fe^{3+}/Fe^{total} ratio in clinopyroxene, which has a relatively large uncertainty when obtained, as is common, from EMP analyses by stoichiometry. Accordingly, a Fe^{3+}/Fe^{total} ratio of 0.30, which is a common intermediate value for clinopyroxene in many eclogites, has been assigned to clinopyroxene in the three eclogite samples. The resulting temperatures (at 35 kbar) are 878°C (EH-25), 853°C (EH-81), and 882°C (Augland et al. 2010), which are consistent with the independent temperature estimates for orthopyroxene eclogite EH-15B (fig. 4).

Regardless of the uncertainty in Grt-Cpx temperatures, it appears that the Tvaerdal eclogites reached peak temperatures of 870°–950°C at pressures of 35–40 kbar (fig. 4), thereby justifying inclusion of the Tvaerdal terrane among the ever-growing number of UHP terranes recognized worldwide.

Eclogite Sm-Nd and Ar-Ar Geochronology. Table 2 lists the rare earth element (REE) concentrations of clinopyroxenes, garnets, and a biotite from HKB-6B as determined by LA-ICP-MS (complete trace element concentrations are listed in table S2). REE concentrations normalized to chondrite are plotted in figure 5*A* and show the characteristic crossed patterns for clinopyroxene and garnet, indicating that these minerals are suitable for dating by the Sm-Nd mineral isochron technique. Figure 5 present two eclogite dates obtained at Lamont-Doherty Earth Observatory. Biotite eclogite HKB-6B (sample locality 4 in fig. 1) yields a Sm-Nd age of 399.7 ± 4.1 Ma (2σ; MSWD = 1.2; fig. 5*B*), and orthopyroxene eclogite EH-15B (locality 2), the eclogite used for geothermobarometry, gives an age of 407 ± 7 Ma (2σ;

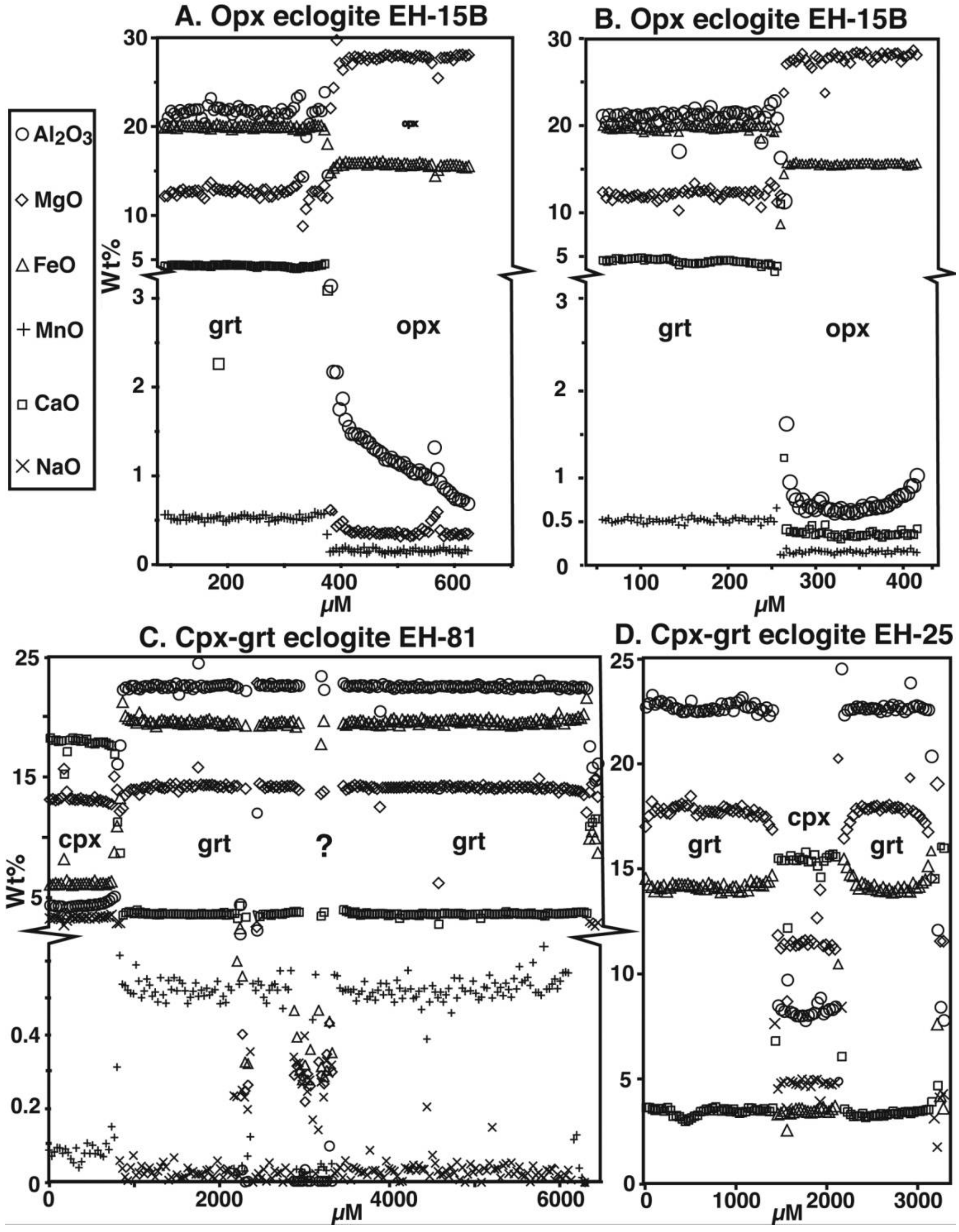

Figure 3. Selected electron microprobe scans across garnet, orthopyroxene, and clinopyroxene in eclogites EH-15B (*A*, *B*), EH-81 (*C*), and EH-25 (*D*). Note the generally flat patterns for most major oxides in mineral cores, with some garnets showing slightly decreasing MgO and increasing FeO at their rims. In contrast, the rimward increase in Al_2O_3 in EH-15B orthopyroxenes is particularly dramatic.

MSWD = 1.02; fig. 5*C*); both are consistent with the eclogite U-Pb ages obtained by Augland et al. (2010), Corfu and Hartz (2011), and this study (see below). The 397.3 ± 1.7 Ma U-Pb age reported by Corfu and Hartz (2011) is from a sample from the same outcrop as EH-15B and is slightly outside the error of the Sm-Nd age at the 2σ level. The dates obtained by Sm-Nd are less precise than the U-Pb ages but have

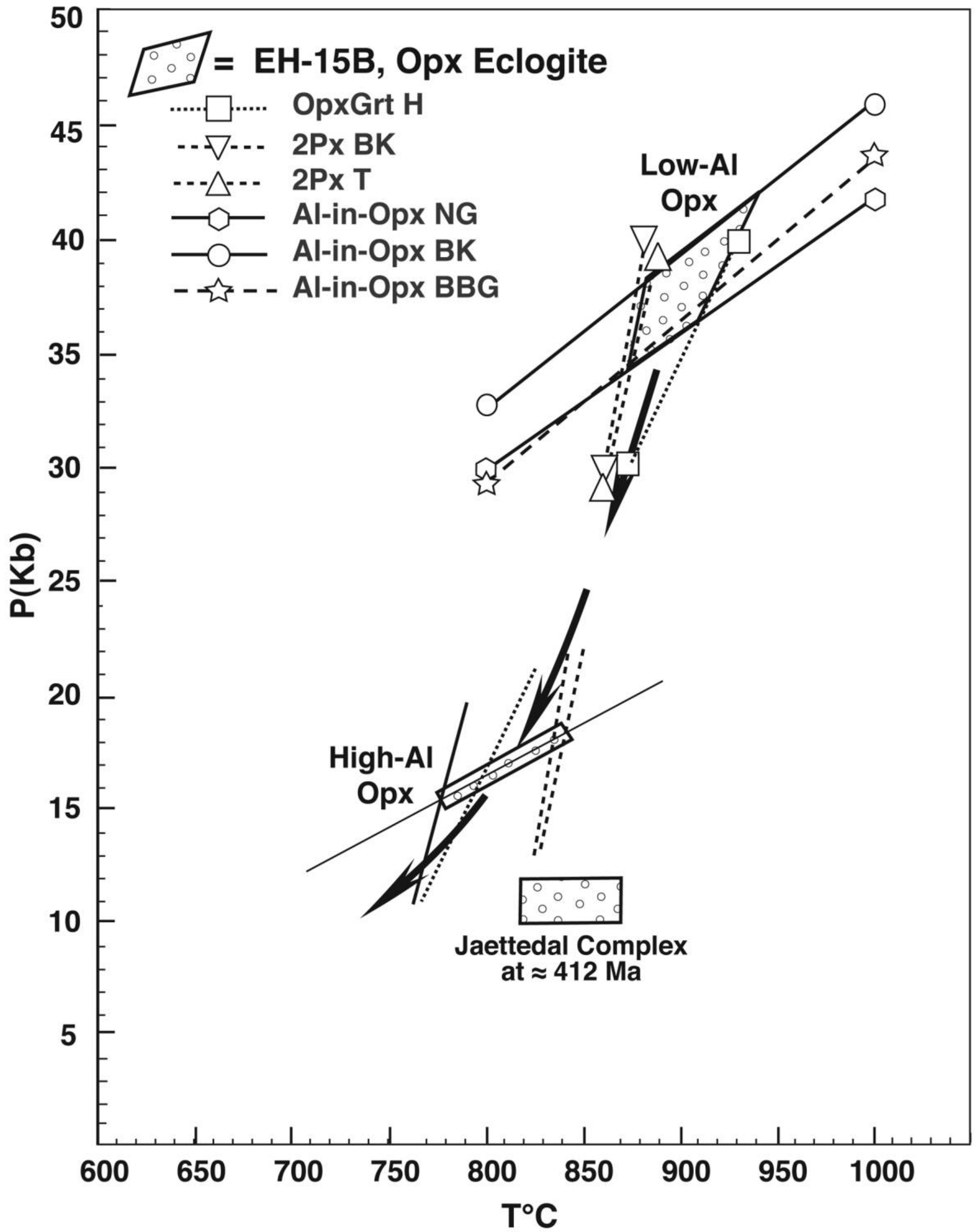

Figure 4. Diagram showing pressure-temperature estimates for eclogite EH-15B and mean temperature estimates using six Grt-Cpx Fe-Mg geothermometers for EH-15B, EH-25, EH-81 (this study), and LEA 06-61 (Augland et al. 2011). See text for references. *PT* estimates for the Jaettedal Complex are from Johnston et al. (2015).

the advantage of directly dating the formation of garnet in the eclogite (Griffin and Brueckner 1980).

Biotite separated from eclogite HKB-6B (also dated by Sm-Nd) and retrograded eclogite HKB-7 were dated by the ^{40}Ar-^{39}Ar step-heating technique at the Argon Geochronology for the Earth Sciences (AGES) laboratory at Lamont-Doherty Earth Observatory. Three individual crystals from HKB-6B give integrated ages of 394.2 ± 0.6, 395.3 ± 0.5, and 411.5 ± 0.5 Ma (1σ; appendix 3). A single crystal

Table 2. Sm, Nd, and Sr Concentrations and Isotopic Compositions from Eclogites EH-15B and HKB-6B

	Sr (ppm)	$^{87}Sr/^{86}Sr$	Sm (ppm)	Nd (ppm)	$^{147}Sm/^{144}Nd$	$^{143}Nd/^{144}Nd$	2σ
ID:							
EH-15B orthopyroxene eclogite:							
cpx1	434	.704668 ± 07	4.13	16.9	.149	.512262	.000008
cpx2	nm	nm	4.07	16.1	.153	.512222	.000008
grt			1.03	.636	.972	.514466	.00001
grt2			1.03	.617	1.01	.514483	.000008
wr			1.65	5.42	.184	.512332	.000008
HKB-6B biotite eclogite:							
cpx1	601	.711083 ± 06	2.52	9.97	.153	.512779	.000008
cpx2	734	.710959 ± 14	2.98	11.9	.151	.512243	.000008
biotite	80.6	.750214 ± 14	.36	1.72	.127	.51217	.00001
grt1			1.16	.764	.92	.51413	.000012
pale grt2			1.11	.738	.906	.514232	.000012
dark grt2			1.13	.749	.916	.514255	.000017
wr2			1.88	5.67	.2	.51238	.00001

	La	Ce	Pr	Nd	Sm	Eu	Gd	Tb	Dy	Ho	Er	Tm	Yb	Lu
LA-ICP-MS:														
HKB-6B biotite eclogite:														
cpx1	3.08	10.7	1.91	9.38	2.49	.712	1.74	.19	.68	.08	.14		.06	.006
cpx2	3.56	13.5	2.31	11	2.94	.871	1.94	.215	.79	.096	.19		.09	.011
biotite	3.39	9.71	1.09	3.74	.75	1.1	.43	.069	.29	.038	.07		.04	.012
grt1	.02	.12	.05	70	1.16	.648	3.75	.782	5.59	1.2	3.37		3.14	.505
grt1b	.01	.09	.05	.71	1.16	.633	3.9	.826	5.75	1.19	3.35		3.19	.513
Normalized to	.329	.855	.13	.63	.203	.077	.276	.051	.343	.077	.225	.035	.22	.339
cpx1	9.36	12.5	14.7	14.9	12.3	9.25	6.32	3.71	1.98	1.04	.62		.29	.19
cpx2	10.8	15.7	17.7	17.4	14.5	11.3	7.02	4.2	2.3	1.24	.85		.4	.31
biotite	10.3	11.35	8.42	5.93	3.68	14.3	1.57	1.35	.841	.494	.33		.17	.35
grt1	.073	.14	.388	1.11	5.7	8.41	13.6	15.3	16.3	15.6	15		14.3	14.9
grt2	.019	.11	.365	1.13	5.72	8.22	14.1	16.2	16.8	15.5	14.9		14.5	15.1

Note. Concentrations were determined by isotope dilution (ID) and by laser ablation inductively coupled plasma mass spectrometry (LA-ICP-MS).

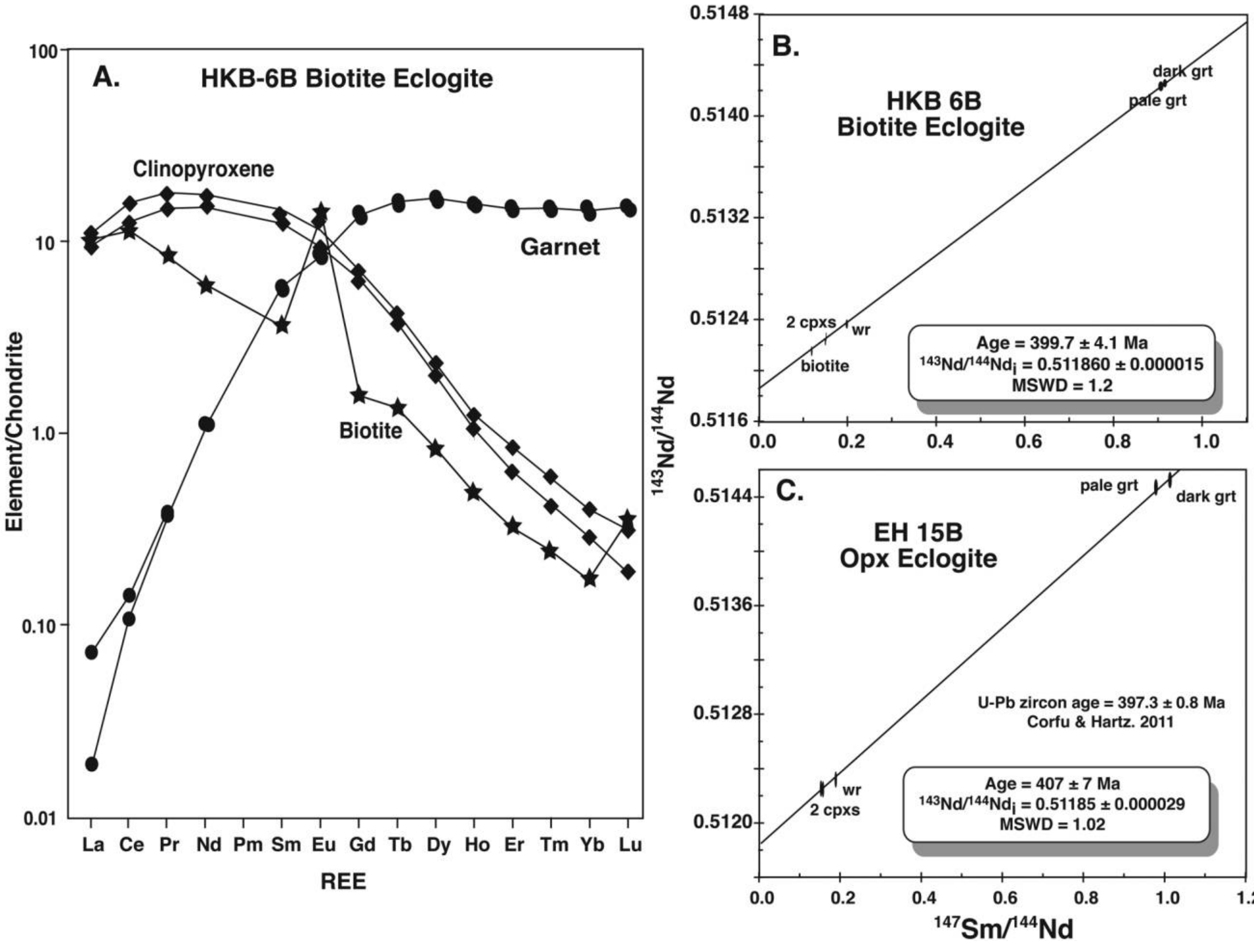

Figure 5. *A*, Laser ablation inductively coupled plasma mass spectrometry rare earth element (REE) clinopyroxene, garnet, and biotite patterns from eclogite HKB-6B. Note the Eu anomaly for biotite, suggesting formation or equilibration in the plagioclase stability field. Ar-Ar ages were obtained from biotite separates. *B*, *C*, Sm-Nd mineral isochron diagrams showing ages from eclogites HKB-6B and EH-15B.

from HKB-7 yielded a plateau of 401.4 ± 0.6 Ma and an integrated age of 401.2 ± 0.5 Ma. The similarity of most of these Ar-Ar ages with those of the other dating schemes is surprising since the Ar-Ar system should have a much lower closure temperature than the U-Pb zircon or Sm-Nd mineral systems. The ages could reflect extremely rapid cooling of the Tvaerdal Complex, but it is more likely that they reflect the presence of excess argon in the eclogites, which resulted in spurious ages that fortuitously coincide with the ages give by the other systems. The older age of one of the biotites (411.5 Ma) is consistent with this hypothesis.

Detrital Mineral Geochronology and Geochemistry

We collected detrital zircon, rutile, and titanite grains from stream sediments just north of the middle lake in Tvaerdal (X in fig. 1) and analyzed them by LA-ICP-MS and multicollector LA-ICP-MS at the Geochemical Analysis Unit, Macquarie University, Sydney. The sampled stream drains the Tvaerdal Complex exclusively, so we assume that all analyzed minerals were derived from it, although contributions from the Jaettedal Complex cannot be excluded entirely. The rutile and titanite results do not provide new information on the geochronology of the Tvaerdal Complex, but the data, figures, and a short discussion are available in appendix 4. The complete zircon data set—which includes all analyzed elements; Pb/Pb, U/Pb, and Th/Pb ratios; the ages determined from these ratios (Pb corrected for discordant ages); and Lu-Hf isotopic results—are available in table S3. Table S4 shortens the data set by focusing on ages, Hf-isotope compositions, selected trace element concentrations, and rock classifications using the classification and regression tree (CART) scheme of Belousova et al. (2002). The zircon data, based on a large number of analyses (89 analyses of 77 zircons), corroborate the previous U-Pb studies by Augland et al. (2010, 2011), Johnston et al. (2010), and Corfu and Hartz (2011) but amplify these studies by providing a statistical basis for addressing some of the issues raised in those studies, including the timing of Scandian metamorphism and melting and whether the Tvaerdal Complex originated as a Baltic or Laurentian terrane. Cathodoluminescence (CL) images of representative zircons are presented in figure 6. CL images of all detrital zircons analyzed are available in figure S2, with U-Pb dates, Hf isotope ratios, and interpreted host rocks.

Proterozoic Age Patterns. All zircons analyzed define two diffuse mixing lines with a Caledonian lower intercept and upper intercepts of ≈1.63 and ≈0.95 Ga when plotted on a standard Concordia diagram (fig. 7*A*). Drawing these Pb-loss chords commonly involves an arbitrary subdivision of the data that fall off Concordia. These ambiguities are partially resolved on a plot of the $^{176}Hf/^{177}Hf$ ratio versus the U/Pb zircon age (fig. 7*B*). Zircons can yield U-Pb ages younger than their time of initial crystallization due to Pb loss during subsequent heating, but zircon Hf isotopic ratios are not likely to change during heating as long as the zircons themselves do not recrystallize. Therefore, the $^{177}Hf/^{176}Hf$ ratio is set at the time of initial zircon crystallization and does not increase significantly through radioactive decay because of the very low amount of parent, Lu, relative to the large amount of daughter, Hf (table S4). Three lines of constant $^{176}Hf/^{177}Hf$ ratio (solid horizontal lines in fig. 7*B*) can be fitted through most of the zircons that have low present-day $^{176}Hf/^{177}Hf$ ratios. This procedure defines a ≈400 Ma Pb-loss event within zircons estimated to have formed at 1.64 ± 0.04, 1.28 ± 0.04, and 1.06 ± 0.05 Ga (ages are highlighted by vertical dashed bands). Further horizontal lines might be fitted through younger zircons, but these zircons could equally well have been zircons >1 Ga old that were partially reset during later thermal events.

All Scandian-aged zircons but one have the negative present-day εHf values characteristic of evolved continental crust. A sloping line (dashed line with arrowhead) shows the possible growth trajectory of the $^{177}Hf/^{176}Hf$ ratios of juvenile continental crust ($^{176}Lu/^{177}Hf$ ratio = 0.02) originally generated from the mantle during magmatism at ≈1.64 Ga. This magmatism is assumed to start with an "average" $^{177}Hf/^{176}Hf$ upper mantle value (i.e., halfway between depleted mantle and chondrite uniform reservoir trajectories). New zircons that crystallized during subsequent events, either within magmas or during metamorphism at 1.28, 1.06, and 0.4 (Scandian) Ga, would be characterized by the progressively increasing $^{177}Hf/^{176}Hf$ ratio of the host rock through time. Many of the zircons that formed after 1.64 Ga plot along or compellingly near the plotted crustal growth trajectory, suggesting that they crystallized from anatectic melts generated by remelting this ≈1.64 Ga continental crust at 1.28, 1.06, and 0.4 Ga. Zircons that crystallized from ≈400 Ma anatectic melts of this crust would plot near the tip of the arrow in figure 7*B*. There are other subtle effects that can be seen on the figure; for example, the cluster of ages between 0.6 and 0.8 Ga could represent further major crustal melting events but more likely reflect partial Pb-loss from older zircons during Scandian metamorphism and melting. Thus, the broad vertical band at ≈400 Ma represents a mixture of ancient zircons with ages completely or nearly completely reset during Scandian metamorphism and/or melting (lower $^{177}Hf/^{176}Hf$ ratios) and newly formed zircons crystallized from magmas generated by melting the ancient crust (higher $^{177}Hf/^{176}Hf$ ratios). The Tvaerdal zircons therefore provide compelling evidence that a significant portion of the Scandian granitoids and migmatites formed by melting of the Proterozoic gneisses and are in fact anatectic granitoids.

Three analyses from zircon 65, which has a $^{207}Pb/^{206}Pb$ age of 1641 Ma, give the lowest $^{177}Hf/^{176}Hf$ ratios measured (average = 0.28161). These ratios give Early Proterozoic/latest Archean model ages when extrapolated toward the mantle evolution curves (fig. 7*B*). It represents the only possible pre–Middle Proterozoic zircon identified to date in the Tvaerdal Complex, in contrast with several Jaettedal zircons that give Paleoproterozoic and Archean U-Pb ages (Johnston et al. 2010).

Trace Element Patterns: Scandian versus Proterozoic Zircons. Table S4 lists the igneous classification of the zircon host rock using the CART "decision tree" of Belousova et al. (2002). Zircons that are listed in these columns as metamorphic ("Scandian Met") or reset igneous ("Reset Ign") grains (see further discussion below) are not appropriate for the application of the Belousova et al. system, which is designed to identify igneous zircons only. The identifications of all zircons, regardless of whether they are igneous, reset igneous, or metamorphic, as well as the trace element concentrations used for their classification are presented in table S3. Only 42 of 81 zircons (and 112 analyses; some grains were analyzed more than once) are identified as igneous, of which 33 originated from granitoids (high, low, and undersaturated SiO_2) and 1 originated from a mafic rock, with the rest (8) giving either ambiguous identifications or different

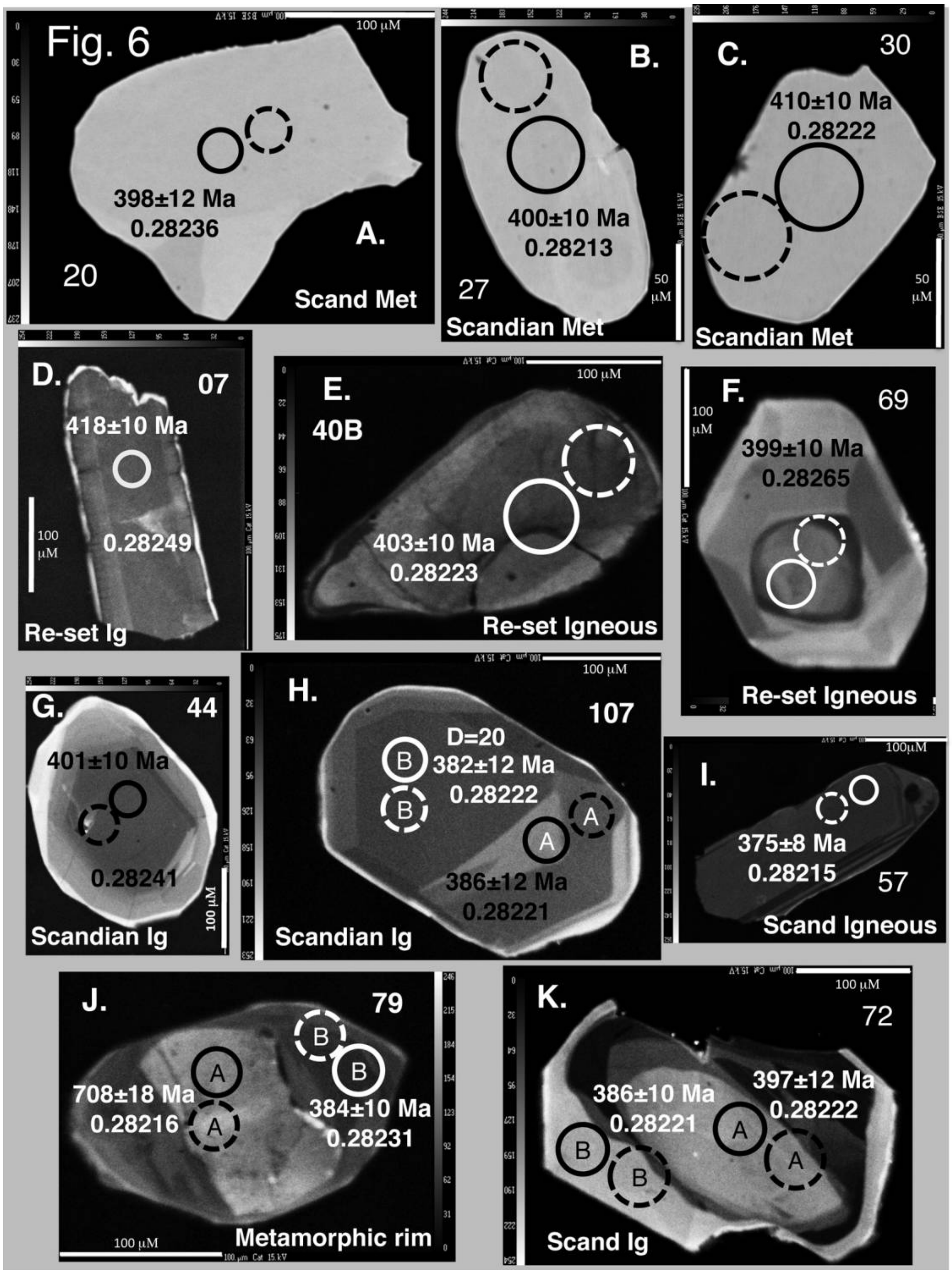

Figure 6. Cathodoluminescence images of representative zircons classified as Scandian metamorphic grains (*A*–*C*), reset Proterozoic igneous grains (*D*–*F*), Scandian igneous prisms (*G*–*I*), and Scandian rims (*J*, *K*). Refer to figure 10 for rare earth element patterns from these classes. A color version of this figure is available online.

identifications depending on which part of the zircon was analyzed. It is not surprising that many Tvaerdal sequence zircons have granitoid signatures, given its abundant granitoid intrusions.

The zircon trace element patterns suggest that many of the granitoids are low in silica, with 11 identified as containing less than 65% SiO_2. Figure 8*A* plots Hf versus Y concentrations (after fig. 9

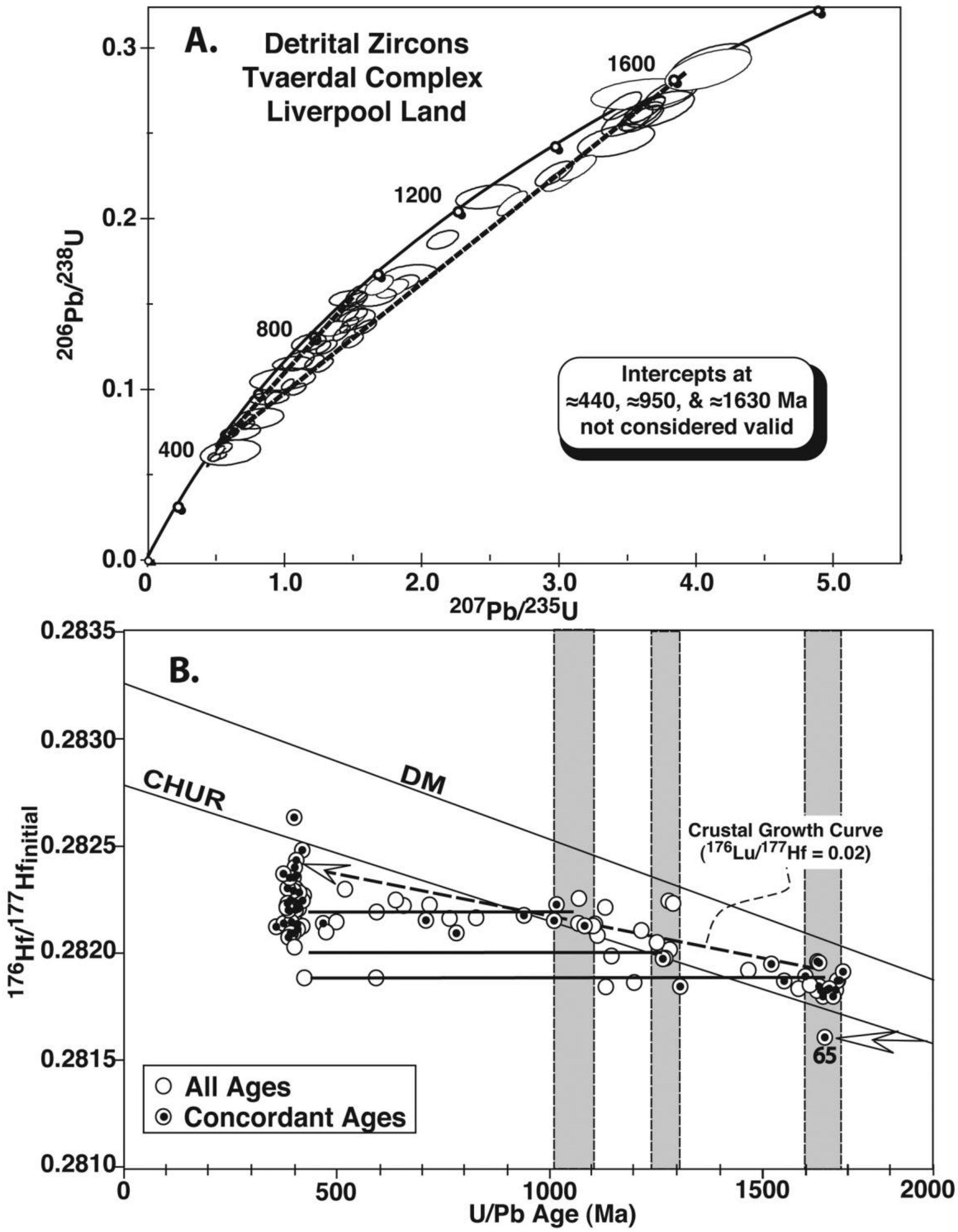

Figure 7. *A*, Concordia U-Pb plot of all zircons analyzed from the Tvaerdal Complex. The intercepts are not believed to define meaningful ages because of the scatter of the data. *B*, $^{238}U/^{206}Pb$ (<1.0 Ga) and $^{207}Pb/^{206}Pb$ (>1.0 Ga) age versus $^{176}Hf/^{177}Hf$ ratio diagram of Tvaerdal zircons. Vertical dashed bands represent best estimates for Proterozoic magmatic events. The sloped dashed line with an arrow shows a possible $^{176}Hf/^{177}Hf$ ratio growth trajectory assuming $^{177}Lu/^{176}Hf$ ratios typical of continental crust (0.02). Horizontal lines show "no-growth" trajectories of zircons formed at ≈1.64, 1.28, and 1.06 Ga. The arrow at the lower right points to the only zircon analyzed with a possible Archean origin. See text for further details. DM = depleted mantle; CHUR = chondrite uniform reservoir.

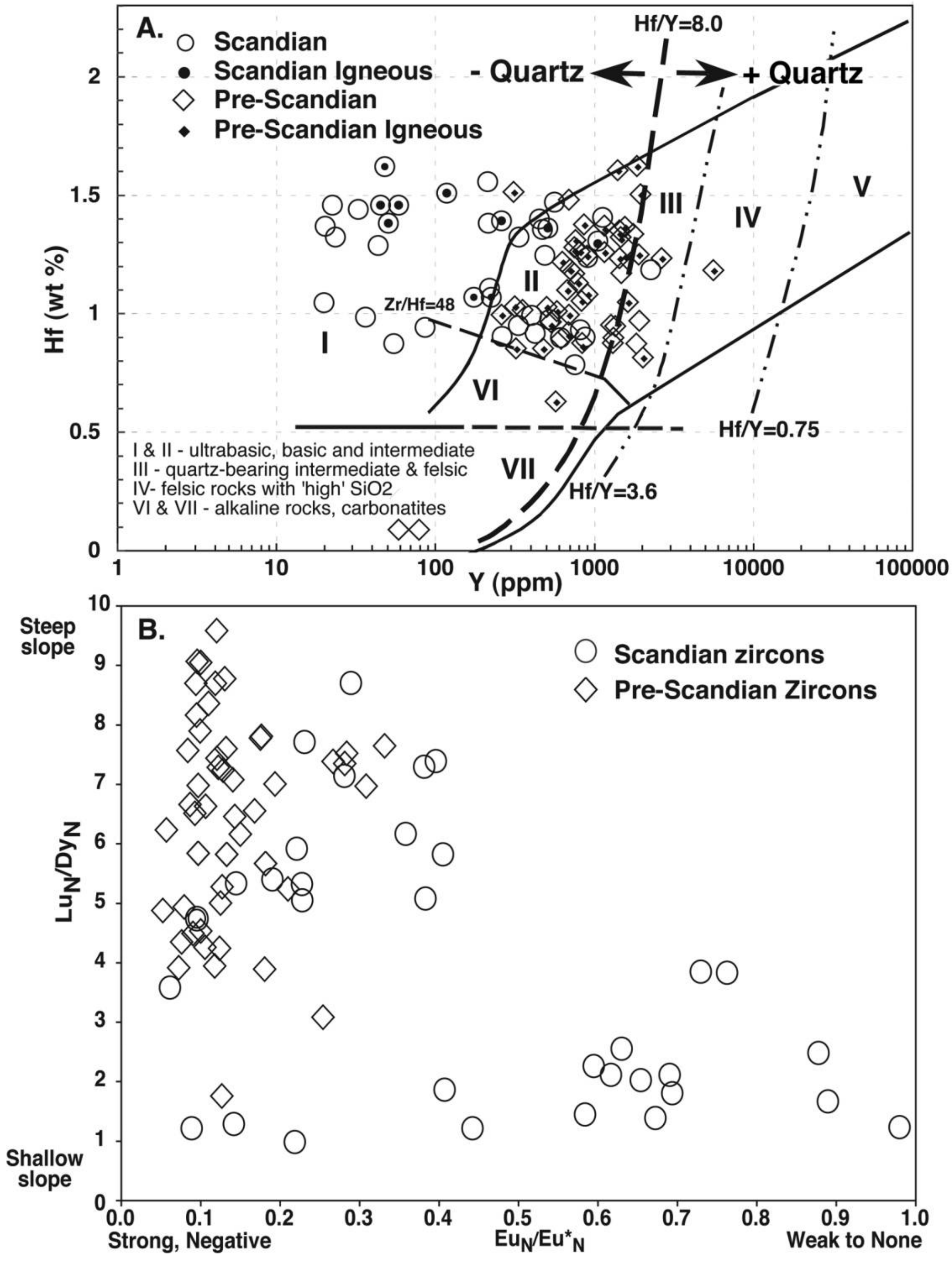

Figure 8. Trace element patterns of Tvaerdal zircons. *A*, All analyses on a Hf versus Y diagram. Filled symbols are zircons believed to have had an igneous origin. Most Precambrian zircons (diamonds) are near or above the quartz present/absent curve, whereas Scandian zircons (circles) are generally quartz-free (based on the Hf/Y ratio). *B*, All analyses on a Lu_N/Dy_N versus (Eu/Eu^*_N) diagram. Note that relatively flat heavy rare earth element slopes ($Lu_N/Dy_N < 4$) are restricted to Scandian-aged zircons, suggesting the involvement of garnet during formation. Strong negative Eu anomalies are restricted to Proterozoic zircons. Many Scandian zircons have weaker anomalies (>0.5), and three with very weak Eu anomalies may have been derived from eclogite or garnet pyroxenite.

of Belousova et al. 2002) of all zircons analyzed, and it can be seen that most analyses that plot well to the left of the boundary between quartz absent (−Quartz) and quartz present (+Quartz) give Scandian ages (shown as circles), while those that plot along or only slightly to the left of the boundary give Precambrian ages (diamonds). Many or most of the Proterozoic zircons from the Tvaerdal sequence were probably derived from granitoid plutons, so their CART identifications are probably broadly correct. However, the Scandian zircons from the Tvaerdal sequence are from metamorphic rocks or melts generated by melting these metamorphic rocks, so it is likely that many of these zircons formed in the presence of garnet. Figure 8*B* illustrates this likely presence of garnet (suggested by shallow Lu/Dy ratios) and absence of plagioclase (suggested by weak Eu anomalies) in the host rocks that generated Scandian melts or were recrystallized during Scandian metamorphism (circles). The presence of garnet complicates the usefulness of the zircon CART decision tree since garnet competes with zircon for many of the elements used in the binary switches when keying down the decision tree ladder (i.e., heavy REEs [HREEs]).

Caledonian Zircon Ages from the Tvaerdal Complex. Thirty nine of 81 zircon analyses yielded $^{206}Pb/^{238}U$ ages that range between 500 and 357 Ma (table S4, fig. 9*A*) and are considered "Caledonian" sensu lato. The remaining Late Proterozoic and early Paleozoic

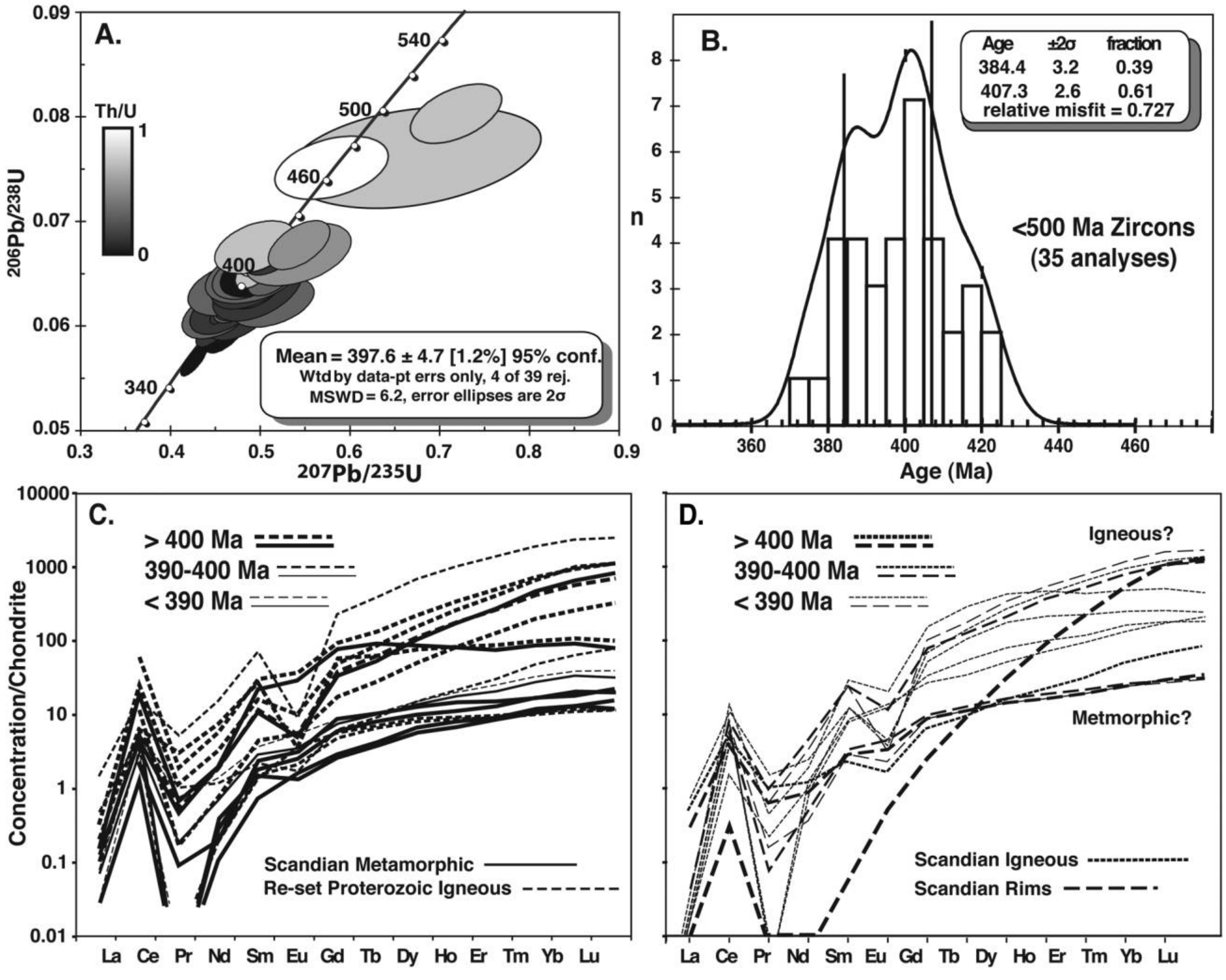

Figure 9. *A*, Concordia plot of zircon U-Pb "Caledonian" ages from the Tvaerdal Complex. Note that most ages >410 Ma are largely discordant. *B*, Age distribution histogram showing a double peak. The older age is interpreted to date peak high-pressure/ultrahigh-pressure metamorphism; the younger age dates anatectic melting. *C*, Chondrite-normalized rare earth element (REE) patterns for zircons classified as metamorphic (solid lines) and reset Proterozoic igneous (dashed lines). *D*, Chondrite-normalize REE patterns for zircons classified as Scandian igneous (dotted lines) and Scandian rims (dashed lines). Both diagrams divide ages into >400 Ma, 390–400 Ma, and <390 Ma.

ages, between 0.98 and 0.5 Ga, are considered mixed ages, the result of partial reequilibration and Pb loss. The rejection of three anomalously old ages of 468, 474, and 498 Ma (discussed further below) and one anomalously young age (357 Ma, zircon 53) from the Tvaerdal Complex leaves a remaining age range from 423 to 374 Ma and an age distribution with two overlapping peaks (fig. 9*B*), one at 407.3 ± 2.6 Ma and another at 384 ± 3.2 Ma (both 2σ). The younger ≈384 Ma age agrees well with thermal ionization MS zircon dates from late to postkinematic granitoids by Corfu and Hartz (2011) and Augland et al. (2010, 2011) but is younger than a 394.5 +13/−8.4 Ma age for a zircon rim from a crosscutting granitic dike within the Jaettedal Complex (Johnston et al. 2010). The older ≈407 Ma age agrees well with our Sm-Nd mineral isochrons (fig. 5) and three TuffZirc ages by Johnston et al. (2010) from zircon rims taken from Tvaerdal gneisses and migmatites. Johnston et al. (2010) interpret these older ages as dating earlier metamorphism. However, they are significantly older than very precise and consistent zircon ages (397.3 ± 1.7, 398.8 ± 1.3, and 398.7 ± 0.9 Ma [2σ] from three different eclogites; Corfu and Hartz 2011), although they are within the error of the 399.5 ± 0.9 Ma eclogite age determined by Augland et al. (2010). Thus, there is some uncertainty on the timing UHP and subsequent HP metamorphism and anatectic melting.

Simple, consistent relationships between zircon geochemistry (CART designations, Eu anomalies, HREE slopes, Th/U ratios, ^{176}Hf/^{177}Hf ratios, etc.) and Scandian ages were not generally observed. However, zircons could be grouped into four broad classes based on morphology, CL characteristics, and, to a lesser extent, REE patterns, and three of these groups give interpretable age patterns, although always with some exceptions. Examples of each class are shown in figure 6, and the classification of all dated zircons is available in figure S2.

"Metamorphic" zircons have amoeboid, oblate, irregular, or only weakly prismatic morphology and gave CL images that are either homogenous (fig. 6*A*–6*C*) or show fuzzy, indistinct zoning. Six of seven have flat HREE patterns, and most lack strong Eu anomalies (fig. 9*C*). Six zircons give concordant ages between 410 and 400 Ma, with an "older" average age of 403.8 ± 3.6 Ma (1σ). Zircon 20 gives a younger age of 398 Ma but is discordant (15%).

"Reset" zircons (fig. 6*D*–6*F*) comprise the least reliable category because of their variable morphologies, CL images, REE patterns, and Eu anomalies (table S4). They are presumed to be Proterozoic zircons that had their U-Pb isotopic system reset to varying degrees during Scandian metamorphism. They are identified by subhedral to euhedral and/or prismatic shapes with obscured igneous CL patterns (oscillatory zoning, sector zoning, etc.), and many of the obtained dates are from cores surrounded by thin to thick homogenous rims. Many have steeply sloping HREE patterns and strong negative Eu anomalies (fig. 9*C*), supporting their igneous origin, but others have flat, low HREE patterns, suggesting the possible presence of garnet during zircon growth or crystallization. The nine "reset" zircons (fig. 9*C*) define a long span of 419–384 Ma, as would be expected if some did not homogenize completely during Scandian thermal events.

"Scandian igneous" zircons are euhdral or prismatic but show distinct, clean igneous CL zoning patters (oscillatory zoning, sector zoning, etc.); lack metamorphic rims; and lack Proterozoic cores (fig. 6*G*–6*I*). All but one is identified as granitoid (table S4) on the basis of the decisions trees of Belousova et al. (2002). Surprisingly, given the abundance of granitoids within the Tvaerdal Complex, there appear to be only six newly formed Scandian igneous zircons (accepting two with discordance >15%), which give ^{238}U/^{206}Pb ages between 397 and 357 Ma (fig. 9*D*) and a narrower range (397–374 Ma) if the 357 Ma age is deleted (henceforth, the 357 Ma age of zircon 53 is considered anomalous).

"Rim" zircons (fig. 6*J*, 6*K*) were grouped into a separate class because homogenous rims are easy to identify regardless of an igneous or metamorphic origin. Like the Scandian igneous zircons, four of five give younger concordant ages (<400 Ma; fig. 9*D*). Most give granitic CART signatures. Zircon 41B, with the older concordant age of 408 Ma, has an igneous REE pattern and a thick rim with a euhedral outline (fig. S2), suggesting relatively early melting (see below). The rest of the zircons presumably grew during retrogression into the amphibolite facies, perhaps expedited by the introduction of water during decompression and possibly, within melts, during the formation of anatectic granitoids (Kohn et al. 2015). There is a tendency toward lower Th/U ratios with decreasing age (fig. 9*A*), consistent with the introduction of water.

Discussion

Scandian Paragenesis of the Tvaerdal Complex. There are two ways of interpreting the ages of the 39 Scandian zircon analyses dated in this study. One is to accept most of the relatively consistent ages determined from three of the four classes described above. Metamorphic zircons define older concordant ^{238}U/^{206}Pb ages between 410 and 400 Ma and are consistent with U-Pb and Sm-Nd ages determined from eclogites. Four (of five) concordant rim ages are younger, between 391 and 384 Ma, consistent with continued zircon growth during retrograde metamorphism. These ages in turn overlap ^{238}U-^{206}Pb dates from zircons believed derived from a Scandian granitoid (389–375 Ma). Reset Proterozoic igneous zircons give the least reliable ages, as would be expected if reequilibration did not result in complete isotopic homogenization, which would explain their wide age range (419–384 Ma) and some of the oldest dates (419 and 418 Ma). Ignoring these zircons suggests that UHP metamorphism occurred between 411 and 398 Ma and that continued metamorphism under decreasing *PT* conditions occurred between 398 and 384 Ma, accompanied and followed by anatectic melting that produced granitoids between 389 and 375 Ma. Apparent exceptions to this sequence could be explained away by the relatively large errors for most ages determined by LA-ICP-MS. For example, the 408 $\pm$ 12 Ma date for the zircon rim with an igneous morphology (sample 41B) overlaps with 396 Ma at the 2σ level.

The alternate approach rejects the exclusion or special pleading of ages that appear to violate the above age patterns, implying there was considerable temporal overlap in the formation of zircons that formed by metamorphic recrystallization, crystallization out of granitoid melts, or thermal reequilibration. A similar situation exists in the WGC of Norway, where zircons U/Pb ages from undeformed plagioclase-bearing dikes overlap the entire range of ages obtained from zircons within eclogites (Kylander-Clark and Hacker 2014). This approach implies that igneous zircons could have formed from melts as early as 408 Ma at the same time as new zircons formed by UHP metamorphic recrystallization and, similarly, that metamorphic zircons continued to form or reequilibrate or form rims as recently as 384 Ma, even as melting and migmatization formed new igneous zircons (Kohn et al. 2015). Given the lack of any objective mechanism for resolving the two end member interpretations, we propose that the age sequence suggested in the first interpretation is essentially correct but also that metamorphism and igneous activity broadly overlapped.

Tvaerdal Proterozoic Age Patterns: Baltic or Laurentian? Johnston et al. (2015) document a Laurentian affinity for the Jaettedal Complex by matching its Caledonian age patterns with those of the HIPC and other Laurentian complexes, such as Milne Land and Renland (Kalsbeek et al. 2008; Rehnström 2010). This match confirms earlier suggestions (Johnston et al. 2010) that the Proterozoic age patterns of the Jaettedal Complex are also similar to ages from Laurentian complexes such as the Krummedal sequence and the Hagar Bjerg thrust sheet (Rex and Gledhill 1981; Higgens et al. 2004). The next question concerns the genesis of the Tvaerdal Complex: Laurentia or Baltica? Johnston et al. (2010) and Augland et al. (2011) determined Mesoproterozoic U-Pb ages of 1.65–1.67 from Tvaerdal zircons that are highly suggestive of a Baltic origin, but some Laurentian terranes have similar or nearly similar ages. Now there are many more U-Pb zircon ages available from both Laurentia and Baltica. Figure 10 contrasts the cumulative distribution curves of Proterozoic zircon ages from the Tvaerdal Complex (fig. 10*A*, data from this study) with representative U-Pb ages from zircon-rich terranes and basins in southern Baltica (fig. 10*B*, 10*C*) and Laurentia (fig. 10*D*, *E*, *F*). The Tvaerdal zircon probability plot shows a very strong peak at ≈400 Ma, which is surprisingly weak in the WGC (fig. 10*C*). The shaded dashed vertical bands represent the best-estimate ages of Proterozoic thermal events, as inferred with the help of Hf isotopes (i.e., ≈1.64, 1.28, and 1.06 Ga; see "Proterozoic Age Patterns"). It can be seen that the 1.64 band is within error of the slightly older peak defined by zircons from Norwegian Siluro-Devonian basins (fig. 10*B*) and lines up very well with the very pronounced 1.6 Ga (Gothian orogeny) peak in the WGC of Norway (fig. 10*C*), but it is also close to peaks from the Krummedal sequence, the Moine sequence, and Greenland Devonian basins (fig. 10*D*–10*F*). The 1.28 Ga band does not line up with any strong peak from either Baltic terrane, but neither does it does line up with the many broad peaks defined by zircon ages from Greenland and Scotland basins. Similarly, the 1.05 Ga peak is within error of peaks from the WGC and Siluro-Devonian basins of Baltica, but it is also within error of a strong peak from the Moine sequences of Scotland and a minor peak from the Krummedal sequence of Greenland, both of which are Laurentian (fig. 10*E*, 10*F*). Some of these mismatches are almost certainly due to significant nonzero Pb loss from Tvaerdal zircons as a result of intense Scandian reheating.

Nevertheless, there are telling differences between Baltic and Laurentian ages. The Moine and Krummedal sequence zircons and zircons from other Greenland basins have several peaks in the Archean and Paleoproterozoic and, in particular except for the Moine sequence, a very strong Mesoproterozoic peak at 1.94–1.95 Ga (thick vertical dashed line). These older ages are absent from Baltic crystalline terranes except in northern Scandinavia (Corfu et al. 2014). Ages older than 1.65 Ga are largely absent in Scandinavia south of ≈65°N (Grimmer et al. 2015). The exceptions are Archean and Early Proterozoic zircons from phyllites beneath

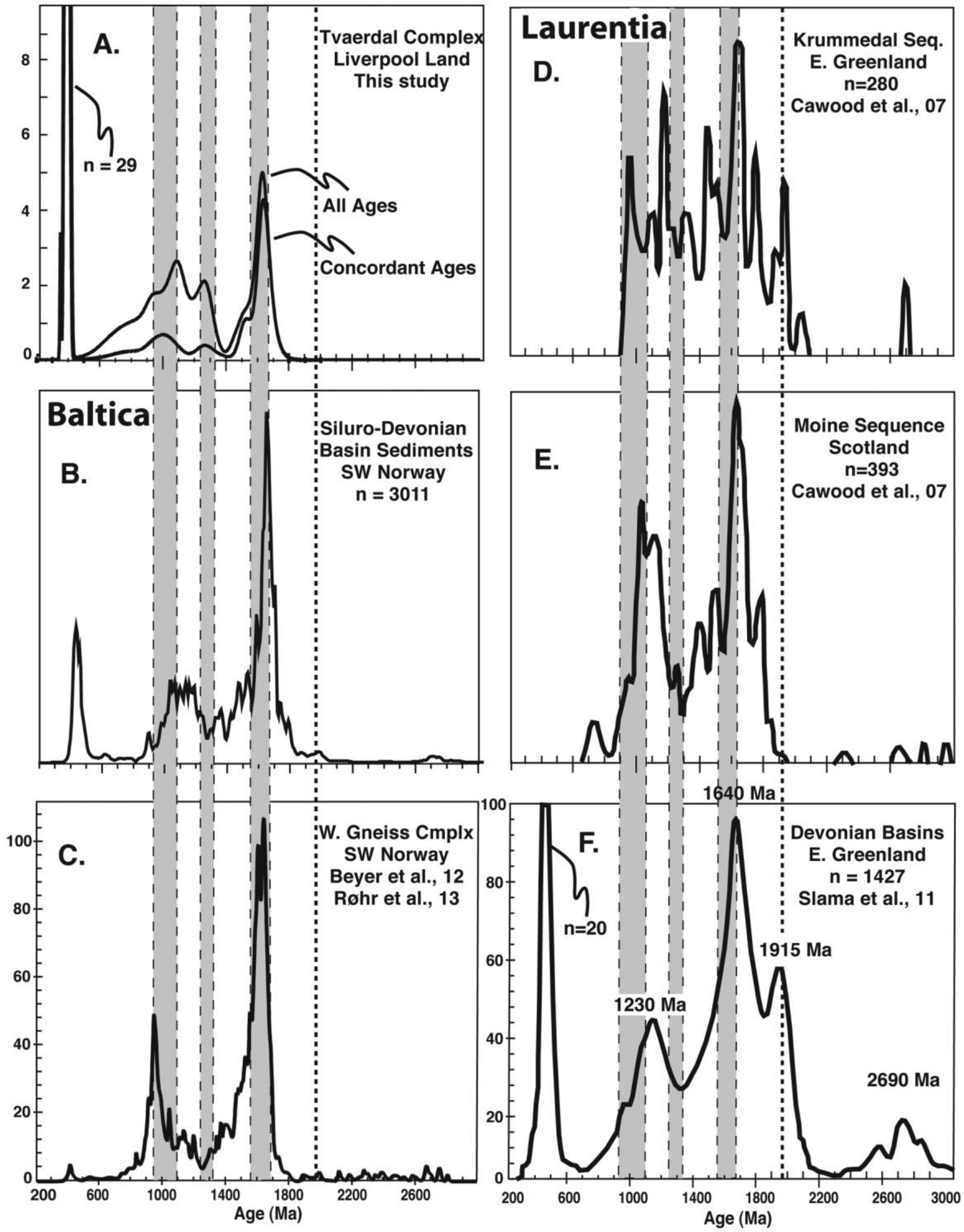

Figure 10. Histograms showing distribution patterns of U-Pb ages of detrital zircons from the Tvaerdal Complex (*A*) and from representative Baltic (*B*, *C*) and Laurentian (*D*–*F*) terranes. Vertical gray bands represent best estimates of Proterozoic magmatic events based on Hf isotope ratios shown in figure 7*B*. Vertical dashed lines show the characteristic 1.74 Ga peak of Laurentian terranes, which is entirely missing in Baltic terranes and the Tvaerdal Complex. Sources are this study (*A*); Pedersen (2011), Templeton (2015), and I. E. Pedersen and J. A. Templeton, unpublished data (*B*); Beyer et al. (2012) and Røhr et al. (2013; *C*); Cawood et al. (2007; *D*, *E*); and Slama et al. (2011; *F*).

south Norway allochthons, but these zircons are accompanied by 0.47–0.8 Ga zircons, which led Slama and Pedersen (2015) to propose derivation from the Archean Timanian orogen in northernmost Scandianvia and Russia. There are also some scattered Archean ages from detrital zircons in a river draining the Almklovdalen peridotite in the WGC, but these zircons probably are derived from the peridotite rather than the enclosing gneisses (Beyer et al. 2012). Finally, Archean zircons occur in sediments of the Hornelen Basin (39 of 1759 analyses) as well as other Devonian and Silurian (Ringerike) basins (Pedersen 2011; Templeton 2015). These zircons may have been sourced in the far north as well, but they also are interpreted as sourced from WGC peridotites (Templeton 2015). In all of these cases, the zircons do not necessarily date crustal events in southern Baltica. None of the zircons from the Tvaerdal Complex gives a Paleoproterozoic or Archean U-Pb age, in clear contrast to the Jaettedal Complex, where these ages are present (Johnston et al. 2010, 2015). This lack of Archean and earliest Proterozoic zircons within the Tvaerdal Complex strengthens arguments for its Baltic origin, probably from south of 65°N (present coordinates).

It should be noted that the pronounced peaks shown in figure 10 do not match up even where they are from adjacent terranes. For example, the Sveconorwegian (≈1 Ga) peaks from the WGC (fig. 10*C*) do not match with most of the peaks from Sveconorwegian basins (fig. 10*B*) immediately to the south of the WGC. Southern Norway is characterized by several assembled Proterozoic terranes (Bamble, Telemark, etc.) of different ages (Bingen et al. 2008), and the WGC may have been equally heterogeneous prior to the Caledonian orogeny. The southern part of the WGC is dominated by Sveconorwegian protolith ages, whereas the northern part is largely Gothian (Brueckner 1979; Tucker et al. 1992; Røhr et al. 2013), attesting to this heterogeneity. So the lack of an exact match of Proterozoic peaks between the WGC and the Tvaerdal Complex should not rule out Baltica, particularly southern Baltica (south of 65°N), as the source of the Tvaerdal Complex.

Paleozoic Age Patterns: Baltic or Laurentian? More compelling evidence for a Baltic provenance is provided by the differences in Paleozoic ages from the Tvaerdal and Jaettedal Complexes (fig. 11). The original division of the metamorphic rocks of Liverpool Land into these two complexes was based on differences in lithology, metamorphic grade, and the presence of eclogite and mantle-wedge peridotite in the Tvaerdal Complex and their absence in the Jaettedal Complex (Johnston et al. 2010). Geochronology confirms this subdivision. Johnston et al. (2010, 2015) document a long Caledonian (sensu lato) but pre-Scandian history at high *PT* for the Jaettedal Complex. This history includes mafic intrusions between 460 and 450 Ma followed by upper amphibolite through granulite-facies metamorphism and migmatization from 440 to 410 Ma. Arguably, the apparent age gap between 450 and 440 Ma may not be statistically significant, in which case the prolonged evolution of the Jaettedal Complex (460–410 Ma, shown as an age distribution diagram in figure 11*A*) matches well with the equally long age span of magmatism responsible for the HIPC (475–415 Ma, shown as circles in fig. 11*A*; data in appendix 4). This match is consistent with the Jaettedal Complex as a Laurentian terrane from the Middle Ordovician to the Early Devonian, probably as the basement to the HIPC during the closure of Iapetus.

Most of the ages from the Tvaerdal Complex (fig. 11*B*) are younger than those from the Jaettedal Complex. Only 9 of 39 Paleozoic ages from the Tvaerdal sequence fall into the Jaettedal age interval (fig. 11*A*), and all but four of these ages are discordant (>15%). Three of the concordant ages (419 ± 10, 418 ± 10, and 411 ± 10 Ma [2σ] for zircons 07, 32B, and 74, respectively) are within error of the youngest age from the Jaettedal Complex (412 ± 5 Ma; Johnston et al. 2015), but given their errors they could equally well be younger (409, 408, and 401 Ma), and the Jaettedal zircon could be older (417 Ma). A second analysis of zircon 32B (i.e., 32A), for example, gives an age of 402 ± 10 Ma. Significantly, only one concordant age (zircon 34, $^{238}U/^{206}Pb$ age = 467 ± 14 Ma) is within error of the beginning of the Jaettedal age span. All four of the Tvaerdal zircons within the 460–410 Ma interval are interpreted as reset Proterozoic zircons. If so, it could be argued that they were not completely reset during Scandian metamorphism. Therefore, while it is impossible to rule out a temporal overlap between the end of metamorphism and melting in the Jaettedal Complex and the beginning of HP/UHP metamorphism in the Tvaerdal Complex, the lack, with one exception, of concordant ages from Tvaerdal zircons within the older range of ages from the Jaettedal Complex (i.e., 460–420 Ma) is considered significant.

The data thus suggest two different evolutions for the two complexes at different pressures, temperatures, and time intervals. The narrow preferred age span for Tvaerdal Complex metamorphism and igneous activity (411–375 Ma) is closer to the interval defined by ages from eclogites and gneisses of the WGC of the Scandinavian Caledonides (≈425–385 Ma;

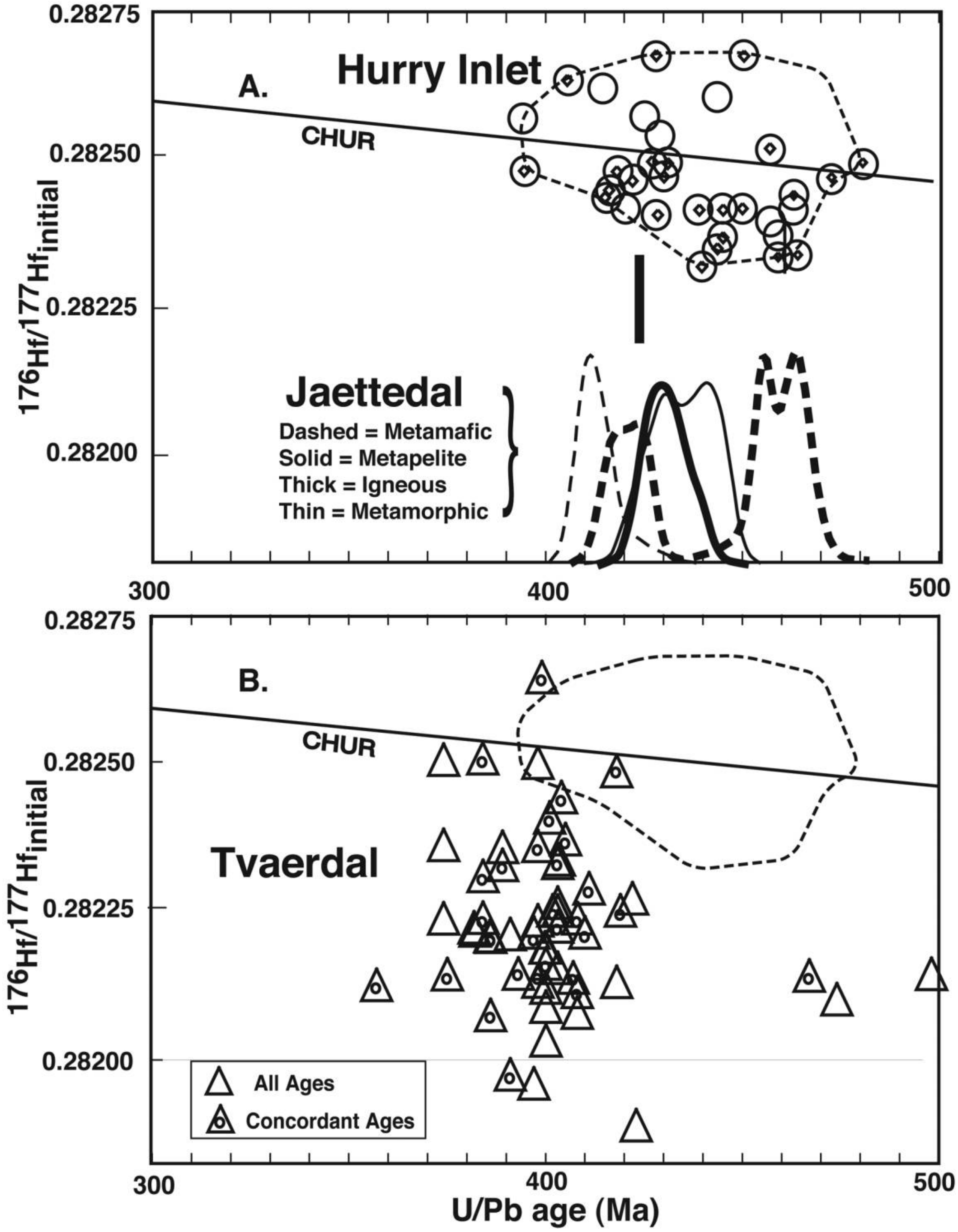

Figure 11. U-Pb age versus Hf isotope diagram contrasting different age patterns of the Hurry Inlet Plutonic Suite (HIPC; *A*) and the Tvaerdal Complex (*B*). Vertical black bars in *A* are from granitoids from Milne Land and Renland (Rehnström 2010). The ages from the HIPC are identical to those of the Jaettedal Complex (shown as a cumulative histogram) and are different from those of the Tvaerdal Complex. Hf isotopes were not measured from the Jaettedal Complex, precluding a more direct comparison. CHUR = chondrite uniform reservoir.

Krogh et al. 2011; Kylander Clark et al. 2012; Gordon et al. 2013), especially if some of the older (410–420 Ma) ages from Tvaerdal zircons are valid. The age spans differ only in the younger ages (389–375 Ma) for zircons from anatectic granitoid of the Tvaerdal Complex, and even here there may be a match based on recent young (down to 385 Ma) U-Pb zircon ages from small, igneous intrusions in the western part of the WGC (Gordon et al. 2013). The paucity of concordant ages >420 Ma from the Tvaerdal Complex therefore argues strongly for a Baltic origin for this complex since it indicates a lack of activity until Scandian collision, as would be expected for a Baltic passive margin approaching an active Laurentian margin.

The similarities in age patterns between the WGC and the Tvaerdal Complex would suggest that they were contiguous prior to Scandian collision, as noted by Augland et al. (2011) and Johnston et al. (2010). Most recent paleomagnetic reconstructions of Scandian collisions place Liverpool Land well north of the WGC (Torsvik et al. 2012; Corfu et al. 2014) roughly 400 m.yr. ago, seemingly contradicting the chronological evidence presented herein. One of us (E. H. Hartz) regards this contradiction as an important objection to the conclusion shared by the rest of us that the Tvaerdal Complex originated from Baltica.

Terrane Transfer Models. The mechanism that transferred the Tvaerdal Complex from Baltica to the base of Laurentia is the subject of several recent publications. Johnston et al. (2010) reviews several underplating models where either the mantle wedge above subducted continental crust is somehow removed, as would be the case for regionally large terranes, or the subducted crust rises through the mantle wedge, which would work only for regionally smaller terranes. Augland et al. (2011, their fig. 5) propose a completely different model where a slice of Baltica is detached along faults from the upper part of Baltica near the end of its exhumation from the mantle and becomes attached to the base of the Laurentian crust. The Ittoqqortoormiit shear zone described by Johnston et al. (2010) separates the Laurentian Jaettedal Complex from the Baltic Tvaerdal Complex and would seem to fit this model. Butler et al. (2011) models the "Liverpool Land Eclogite Terrane" (i.e., the Tvaerdal Complex) as a rising buoyant plug that, instead of returning to the "prowedge" (Baltica), turns in the opposite direction and thrusts over the "retrowedge" (Laurentia). The latter case would have occurred if the Laurentian crust formed a weak backstop, as probably was the case since it was preheated during the subduction of Iapetus. Again, the Ittoqqortoormiit shear zone could have been a suture that juxtaposed the two terranes except that mapping shows the Tvaerdal Complex to be beneath the Jaettedal Complex (Johnston et al. 2010, 2015) instead of on top, as required by the model.

We present another hypothesis, namely, that the Tvaerdal Complex rose through the mantle wedge and underplated Laurentia as a crustal diapir (Yin et al. 2007). This hypothesis is based the presence of abundant red, K-feldspar-bearing granitoid dikes within the Tvaerdal Complex (fig. 2*A*). It would also explain the intense peak at ≈400 Ma defined by U-Pb zircon ages from the Tvaerdal Complex, which contrasts with the very weak 400 Ma peak defined by zircons from the WGC (compare fig. 10*A* and fig. 10*C*). The high $^{177}Hf/^{176}Hf$ ratios of many zircons presumably derived from these granitoids are consistent with formation by anatectic melting of the host Proterozoic gneisses and field observations that show a gradation from banded gneisses to nebulitic and stromatic migmatites to strongly deformed granitoids and finally to undeformed dikes that crosscut all Scandian structures, including the Gubbedalen shear zone. In contrast, the WGC was believed until recently to have undergone limited, if any, melting during the Scandian orogeny. Undeformed granitoids are abundant in the WGC, but geochronology shows that most of them are Proterozoic in age (Brueckner 1979; Tucker et al. 1992; Røhr et al. 2013; Kylander-Clark and Hacker 2014) but escaped Scandian recrystallization (aka "Caledonization"). However, recent publications show that Scandian granitoids do exist (i.e., Labrousse et al. 2004; Krogh et al. 2011; Gordon et al. 2013; Kylander-Clark and Hacker 2014; DesOrmeau et al. 2015) as leucosomes, interboudin melts, and crosscutting pegmatites. At present, these intrusions appear to be limited in extent and occur only in the most deeply subducted portion of the WGC.

The exhumation of a HP/UHP terrane is usually modeled as a coherent return toward the surface along the same route taken during subduction either through "eduction" or "extrusion" (Brueckner and Cuthbert 2013; fig. 1). This return allows the HP/UHP terrane to return to the surface without having to move through the hot core of the overlying mantle wedge. Heating from outside during exhumation is therefore unlikely, and melting should be limited if it occurs at all. An exception to limited melting could occur in a thick terrane such as the WGC (>30 km), which would undergo limited conductive heat loss to the cooler adjacent mantle because of its great thickness (see thermal modeling by Root et al. 2005; see also Hacker 2007). And indeed most exhumation calculations for the WGC indicate that it did not cool significantly from its maximum *PT* conditions of 3.5 GPa and 800°C until it reached midcrustal levels (Cuthbert et al. 2000; Carswell et al. 2003; Labrousse et al. 2004; Root 2005; Hacker 2007), which would explain the existence of Scandian melts in its most deeply subducted portion. However, a thin (10–30 km) terrane that moves back up the subduction channel should do the opposite and "freeze" to temperatures <700°C by the diffusion of heat into the cooler mantle before exhumation to a depth as shallow as 30 km (Root et al. 2005). Thus, a thick HP/UHP terrane should melt to at least some extent during exhumation up the subduction channel, whereas a thin terrane should not.

The areal extent and thickness of the Tvaerdal Complex (present surface exposure, <700 km^2) is unknown since its lower contact is covered by fjords (fig. 1). If it is considerably larger and thicker than suggested by present exposure, the terrane transfer models presented by Augland et al. (2011) and Butler et al. (2011) might be adequate to explain the presence of abundant granitoids within it. But if it is as small as present exposure suggests, a different model is required to explain how it would retain heat or even gain enough heat to cause it to melt so pervasively. The relamination models proposed by Hacker et al. (2011) and Hacker and Gerya (2013) and modeled by Sizova et al. (2012; particularly model IV, fig. 13) might be appropriate. They model a transmantle diapir composed of lower-plate crustal material that moves upward through the mantle wedge to the base of the crust of the upper plate. The combination of small terrane size and a journey through the hot core of the Laurentian mantle wedge would have allowed the Tvaerdal Complex to maintain much of its initial high temperature so that decompression melting became more likely, particularly when H_2O was added late during its retrograde (amphibolite-facies) history. Thermobarometric estimates from this study suggest that cooling was limited during early exhumation with a relatively small decrease in temperature (≈90°C) during a relatively large decrease in pressure (≈21 kbar). Precise titanite and rutile U-Pb ages from the Tvaerdal Complex are between 388 and 380 Ma (Augland et al. 2011; Corfu and Hartz 2011), indicating that temperatures within the Tvaerdal Complex had dropped to only 700°–650°C (the blocking temperatures of titanite and rutile in the WGC; Kylander-Clark et al. 2008) between 410–398 Ma and 388–380 Ma, a range of 10 to 30 m.yr. Thus, a large part of the temperature history during exhumation is between ≈900 and ≈675°C (average values), well within the range of anatectic decompression melting of granitoid gneisses in the presence of H_2O. The validity of our proposed model rests on a small terrane size for the Tvaerdal Complex. Future seismological and gravitational studies may resolve the size issue.

Conclusions

A geochronological and thermobarometric study of eclogites from the Tvaerdal Complex of Liverpool Land, southern Greenland Caledonides, indicates that the complex underwent UHP metamorphism (870°–950°C at pressures of 35–40 kbar) during, before, and after ≈400 Ma, essentially the same time and under the same peak conditions that HP/UHP metamorphism occurred in the WGC of the Norwegian Caledonides. A largely morphological division of Scandian detrital zircons of the Tvaerdal Complex into metamorphic grains, metamorphic and/or igneous rims, Scandian igneous prisms, and reset Proterozoic igneous zircons suggest that UHP metamorphism of the Tvaerdal Complex of the Liverpool Land Eclogite Terrane occurred between 411 and 398 Ma, with some ages suggesting a possible, but less likely, earlier beginning between 410 and 420 Ma. Metamorphism continued under decreasing *PT* conditions, between 398 and 384 Ma, overlapped and followed by a period of anatectic melting that produced granitoids between 389 and 375 Ma. Exceptions to these ages for some zircons suggest considerable overlap in the timing of metamorphism and melting.

The protolith hosts for many Tvaerdal zircons were ≈1.64, 1.28, and 1.06 Ga Proterozoic granitoids, but it is difficult to decide on the basis of these dates whether these granitoids were part of Baltica, generated during the Gothian and Sveconorwegian orogenies, or Laurentia, generated during the Labradoran and Grenville orogenies. However, none of the analyzed zircons from the Tvaerdal Complex, including those described in the literature, give the Archean and 1.75 Proterozoic ages that characterize many Laurentian terranes. In addition, the ages provide little evidence for magmatic or metamorphic events between 470 and 410 m.yr., when the eastern margin of Laurentia was the site of an active continental arc complex. In contrast, the adjacent Jaettedal Complex contains abundant evidence of high-temperature thermal activity during this interval (Johnston et al. 2015). This discrepancy is consistent with the Tvaerdal Complex originally comprising the western edge of the Baltica passive margin, while the Jaettedal Complex was part of the active eastern margin of Laurentia.

Available data suggest that the Tvaerdal Complex and the WGC had similar mantle residence times and were exhumed and cooled at comparable rates, but their apparent different sizes and different degrees of melting require different exhumation mechanisms. We suggest that the Tvaerdal Complex, if it is as small as suggested by present exposure, passed diapirically through the hot mantle wedge and underplated Laurentia, whereas the much thicker and more extensive WGC (>70,000 km^2; Hacker 2007) returned and thrust over Baltica along a cooler trajectory by reversing its subduction path through either eduction or forceful intrusion. The large size of the WGC enabled it to retain much of its heat during exhumation, whereas the possibly much smaller Tvaerdal Complex retained or possibly gained heat by passing through the hotter mantle wedge environment. This journey may explain the high degree of migmatization and anatectic melting that appears to characterize the Tvaerdal Complex (as well as the large number of zircons that give Scandian ages). This study strengthens arguments by Augland et al. (2010, 2011) and Johnston et al. (2010, 2015) that it is an orphaned Baltic terrane that detached from the subducted Baltic crust and embedded itself into the lower crust of the Greenland Caledonides. It is worth noting that, more or less simultaneously, part of the overriding plate (Laurentia) was detached and left behind as the uppermost allochthon of the Scandinavian Caledonides (Agyei-Dwarko et al. 2012). Each plate left part of itself on opposite sides of the Atlantic.

ACKNOWLEDGMENTS

H. K. Brueckner and S. M. Johnston are grateful to E. Hartz, who invited us to field excursions in Liverpool Land in the summers of 2006 and 2007 with expenses covered by Statoil and equipment provided by him. We thank L. Mehl and K. Agustsson for assistance with fieldwork and A. Lynge for assistance with field logistics. We are also very grateful to many people who supported this research and helped us acquire and manipulate the data presented herein, specifically, S. O'Reilly and N. Pearson (Macquarie University), J. Gross and K. Flores (American Museum of Natural History), and T. Plank and L. Bolge (Lamont-Doherty Earth Observatory). This research was supported by City University of New York Faculty Research Award grants 66287-00 35, 67663-00 36, and 68556-00 37 to H. K. Brueckner and by National Science Foundation Division of Earth Sciences grant 08-38530 to H. K. Brueckner and S. M. Johnston. This is contribution 8005 of the Lamont-Doherty Earth Observatory of Columbia University, contribution 812 of the Australian Research Council Centre of Excellence for Core to Crust Fluid Systems (http://www.ccfs.mq.edu.au/), and contribution 1080 of the Geochemical Evolution and Metallogeny of Continents Key Centre (http://www.gemoc.mq.edu.au/).

REFERENCES CITED

Agyei-Dwarko, N. Y.; Augland, L. E.; and Andresen, A. 2012. The Heggmovatn supracrustals, North Norway—a late Mesoproterozoic to early Neoproterozoic (1050–930) terrane of Laurentian origin in the Scandinavian Caledonides. Precambrian Res. 212–213:245–262.

Ai, Y. 1994. A revision of the garnet-clinopyroxene Fe^{2+}-Mg exchange geothermometer. Contrib. Mineral. Petrol. 115: 467–473.

Andersen, T. B.; Jamtveit, B.; Dewey, J. F.; and Swensson, E. 1991. Subduction and eduction of continental crust: major mechanisms during continent-continent collision and orogenic extensional collapse, a model based on the southern Norwegian Caledonides. Terra Nova 3:303–310.

Augland, L. E. 2007. The Gubbedalen shear zone: a terrane boundary in the East Greenland Caledonides; a structural and geochronological study. MSc thesis, University of Oslo, Oslo.

Augland, L. E.; Andresen, A.; and Corfu, F. 2010. Age, structural setting, and exhumation of the Liverpool Land eclogite terrane, East Greenland Caledonides. Lithosphere 2:267–286.

———. 2011. Terrane transfer during the Caledonian orogeny: Baltican affinities of the Liverpool Land Eclogite Terrane in East Greenland. J. Geol. Soc. 168:15–26. doi: 10.1144/0016-76492010-093.

Augland, L. E.; Andresen, A.; Corfu, F.; and Daviknes, H. K. 2012. Late Ordovician to Early Silurian ensialic magmatism in Liverpool Land, East Greenland: new evidence extending the northeastern branch of the continental Laurentian magmatic arc. Geol. Mag. 149: 561–577.

Belousova, E. A.; Griffin, W. L.; O'Reilly, S. Y.; and Fisher, N. I. 2002. Igneous zircon: trace element composition as an indicator of source rock type. Contrib. Mineral. Petrol. 143:602–622. doi:10.1007/s00410-002-0364-7.

Beyer, E. E.; Brueckner, H. K.; Griffin, W. L.; and O'Reilly, S. Y. 2012. Laurentian provenance of Archean mantle fragments in Proterozoic Baltic crust of the Norwegian Caledonides. J. Petrol. 53:1357–1383. doi:10.1093/petrology/egs019.

Bingen, B.; Davis, W. J.; Hamilton, M. A.; Engvik, A. K.; Stein, H. J.; Øyvind, S.; and Øystein N. 2008. Geochronology of high-grade metamorphism in the Sveconorwegian belt, S. Norway: U-Pb, Th-Pb and Re-Os data. Nor. J. Geol. 88:13–42.

Bowman, D. R. 2008. Exhumation history of Caledonian eclogites in Liverpool Land, East Greenland, and

comparison with eclogites in Norway. MSc thesis, University of Auburn, Auburn, Alabama. http://etd.auburn.edu/etd/handle/10415/1109.
Brey, G. P.; Bulatov, V. K.; and Girnis, A. V. 2008. Geobarometry for peridotites: experiments in simple and natural systems from 6 to 10 GPa. J. Petrol. 49:3–24.
Brey, G. P., and Köhler, T. 1990. Geothermobarometry in four-phase lherzolites. II. New thermobarometers, and practical assessment of existing thermobarometers. J. Petrol. 31:1352–1378.
Brueckner, H. K. 1979. Precambrian ages from the Geiranger-Tafjord-Grotli area of the basal gneiss region, southwestern Norway. Norsk Geol. Tidsskr. 59: 141–153.
Brueckner, H. K., and Cuthbert, S. L. 2013. Extension, disruption and translation of an orogenic wedge by exhumation of large ultrahigh pressure terranes: two examples from the Norwegian Caledonides. Lithosphere 5:277–289. doi:10/1130/L256.1.
Brueckner, H. K., and Van Roermund, H. L. M. 2004. Dunk tectonics: a multiple subduction/eduction model for the evolution of the Scandinavian Caledonides. Tectonics 23:TC2004. doi:10.1029/2003TC001502.
Buchanan, W. 2008. Tectonic evolution of a Caledonian aged continental basement eclogite terrane in Liverpool Land, East Greenland. MSc thesis, University of Auburn, Auburn, Alabama. http://etd.auburn.edu/etd/handle/10415/1112.
Butler, J. P.; Beaumont, C.; and Jamieson, R. A. 2011. Crustal emplacement of exhuming (ultra)high-pressure rocks: will that be pro- or retro-side? Geology 39:635–638.
Carswell, D. A.; Brueckner, H. K.; Cuthbert, S. J.; Mehta, K.; and O'Brien, P. J. 2003. The stabilization and the exhumation rate for ultra-high pressure rocks in the Western Gneiss Region of Norway. J. Metamorph. Geol. 21:601–612.
Cawood, P. A.; Nemchin, A. A.; Strachan, R.; Prave, T.; and Krabbendam, M. 2007. Sedimentary basin and detrital zircon record along East Laurentia and Baltica during assembly and breakup of Rodinia. J. Geol. Soc. Lond. 164:257–275.
Cheeney, R. F. 1985. The plutonic igneous and high-grade metamorphic rocks of southern Liverpool Land, central East Greenland, part of a supposed Caledonian and Precambrian complex. Grøn. Geol. Unders. Rapp. 123.
Coe, K. 1975. The Hurry Inlet granite and related rocks of Liverpool Land, East Greenland. Bull. Grønl. Geol. Unders. 115:1–34.
Corfu, F.; Andersen, T. B.; and Gasser, D. 2014. The Scandianvian Caledonides: main features, conceptual advances and critical questions. *In* Corfu, F.; Gasser, D.; and Chew, D. M., eds. New perspectives on the Caledonides of Scandinavia and related areas. Geol. Soc. Spec. Publ. 390:9–43.
Corfu, F., and Hartz, E. H. 2011. U-Pb geochronology in Liverpool Land and Canning Land, East Greenland—the complex record of a polyphase Caledonian orogeny. Can. J. Earth Sci. 48:473–494. doi:10.1139/E10-066.
Cuthbert, S. J.; Carswell, D. A.; Krogh-Ravna, E.; and Wain, A. 2000. Eclogites and eclogites in the Western Gneiss Region, Norwegian Caledonides. Lithos 52: 165–195. doi:10.1016/S0024-4937(99)00090-0.
de Capitani, C., and Petrakakis K. 2010. The computation of equilibrium assemblage diagrams with Theriak/Domino software. Am. Mineral. 95:1006–1016.
DesOrmeau, J. W.; Gordon, S. M.; Kylander-Clark, A. R. C.; Bowring, S. A.; Schoene, B.; and Samperton, K. M. 2015. Insights into (U)HP metamorphism of the Western Gneiss Region, Norway: a high-spatial resolution and high-precision zircon study. Chem. Geol. 414:138–155.
Ganguly, J.; Cheng, W.; and Tirone, T. 1996. Thermodynamics of aluminosilicate garnet solid solution: new experimental data, an optimized model, and thermometric calculations. Contrib Mineral Petrol 126:137–151.
Gasser, D. 2014. The Caledonides of Greenland, Svalbard and other arctic areas: status of research and open questions. *In* Corfu, F.; Gasser, D.; and Chew, D. M., eds. New perspectives on the Caledonides of Scandinavia and related areas. Geol. Soc. Spec. Publ. 390: 93–129. http://dx.doi.org/10.1144/SP390.17.
Gee, D. G.; Janák, M.; Majka, J.; Robinson, P.; and van Roermund, H. 2012. Subduction along and within the Baltoscandian margin during closing of the Iapetus Ocean and Baltica-Laurentia collision. Lithosphere 5: 169–178.
Gilotti, J. A., and Elvevold, S. 2002. Extensional exhumation of a high-pressure granulite terrane in Payer Land, Greenland Caledonides. J. Metamorph. Geol. 21:49–63.
Gilotti, J. A., and McClelland, W. C. 2007. Characteristics of, and a tectonic model for, ultrahigh-pressure metamorphism in the overriding plate of the Caledonian orogen. Int. Geol. Rev. 49:777-797.0020-6814/07/949/777-21.
Gordon, S. M.; McClelland, W. C.; Teyssier, C.; and Fossen, H. 2013. U-Pb dates and trace element geochemistry of zircon from migmatite, Western Gneiss Region, Norway: significance for history of partial melting in continental subduction. Lithos 170/171:35–53.
Griffin, W. L., and Brueckner, H. K. 1980. Caledonian Sm-Nd ages and a crustal origin for Norwegian eclogites. Nature 285:319–321.
Grimmer, J. C.; Hellström, F. A.; and Greiling, R. O. 2015. Traces of the Transscandinavian Igneous Belt in the central Scandinavian Caledonides: U-Pb zircon dating and geochemistry of crystalline basement rocks in the middle allochthon. GFF. doi:10.1080/11035897.2015.1063537.
Hacker, B. R. 2007. Ascent of the ultrahigh-pressure Western Gneiss Region, Norway. *In* Cloos, M.; Carlson, W. D.; Gilbert, M. C.; Liou, J. G.; and Sorensen, S. S., eds. Convergent margin terranes and associated regions: a tribute to W. G. Ernst. Geol. Soc. Am. Spec. Pap. 419:171–184.
Hacker, B. R.; Andersen, T. B.; Johnston, S. M.; Kylander-Clark, A. R. C.; Peterman, E. M.; Walsh, E. O.; and Young, D. 2010. High-temperature deformation dur-

ing continental-margin subduction and exhumation: the ultrahigh-pressure Western Gneiss Region of Norway. Tectonophysics 480:149–171. doi:10.1016/j.tecto.2009.08.012.

Hacker, B. R., and Gerya, T. V. 2013. Paradigms, new and old, for ultrahigh-pressure tectonism. Tectonophysics 603:79–88.

Hacker, B. R.; Kelemen, P. B.; and Behn, M. D. 2011. Differentiation of the continental crust by relamination. Earth Planet. Sci. Lett. 307:501–516.

Hansen, B. T., and Friderichsen, J. D. 1987. Isotopic age dating in Liverpool Land, East Greenland. Geol. Surv. Greenl. Rep. 134:25–37.

Hansen, B. T., and Steiger, R. H. 1971. The geochronology of the Scoresby Sund area. Rapp. Grøn. Geol. Undersøg. 37:55–7.

Harley, S. L. 1984. An experimental study of the partitioning of Fe and Mg between garnet and orthopyroxene. Contrib Mineral Petrol 86:359–373.

Hartz, E.; Andresen, A.; Hodges, K. V.; and Martin, M. W. 2001. Syncontractional extension and exhumation of deep crustal rocks in the East Greenland Caledonides. Tectonics 20:58–77.

Hartz, E. H.; Condon, D.; Austrheim, H.; and Erambert, M. 2005. Rediscovery of the Liverpool Land eclogites (central East Greenland): a post supra-subduction UHP province. Abstract, Mitt. Öster. Mineral. Gesell. 150.

Hartz, E. H.; Podladchikov, Y. Y.; and Dabrowski, D. 2007. Tectonic and reaction overpressures: theoretical models and natural examples. Geophys. Res. Abstr. 9. EGU 2007-A-10430.

Henriksen, N. 2003. Caledonian orogen, East Greenland 70°–82°N. Geol. Surv. Den. Greenl. Geological Map, scale 1 : 1,000,000.

Higgens, A. K.; Elvevold, S.; Escher, J. C.; Frederiksen, K. S.; Gilotti, J. A.; Henriksen, N.; Jepsen, H. F.; et al. 2004. The foreland-propagating thrust architecture of the East Greenland Caledonides, 72°–75°N. J. Geol. Soc. Lond. 161:1009–1026.

Johnston, S. M.; Hartz, E. H.; Brueckner, H. K.; and Gehrels, G. E. 2010. U-Pb zircon geochronology and tectonostratigraphy of southern Liverpool Land, East Greenland: implications for deformation in the overriding plates of continental collisions. Earth Planet. Sci. Lett. 297:512–524.

Johnston, S. M., and Kylander-Clark, A. R. C. 2013. Discovery of an Eo-Meso-Neoarchean terrane in the East Greenland Caledonides. Precambrian Res. 235:295–302.

Johnston, S. M.; Kylander-Clark, A.; and Brueckner, H. K. 2015. Protracted high-temperature metamorphism of the Jaettedal Complex, Liverpool Land, East Greenland: implications for the tectonic evolution of the Caledonian orogenic hanging wall. J. Metamorph. Geol. 33:1025–1046. doi:10.1111/jmg.12167.

Jones, K. A., and Strachan, R. A. 2000. Crustal thickening and ductile extension in the NE Greenland Caledonides: a metamorphic record from anatectic pelites. J. Met. Geol. 18:719–735.

Kalsbeek, F. 1995. Geochemistry, tectonic setting, and poly-orogenic history of Paleoproterozoic basement from the Caledonian fold belt of North-East Greenland. Precambrian Res. 72:301–315.

Kalsbeek, F.; Higgins, A. K.; Jepsen, H. F.; Frei, R.; and Nutman, A. P. 2008. Granites and granites in East Greenland Caledonides. *In* Higgins, A. K.; Gilotti, J. A.; and Smith, M. P., eds. The Greenland Caledonides: evolution of the northeast margin of Laurentia. Geol. Soc. Am. Mem. 202:227–249.

Kohn, M. J.; Corrie, S. L.; and Markley, C. 2015. The fall and rise of metamorphic zircon. Am. Mineral. 100: 897–908. http://dx.doi.org/10.2138/am-2015-5064.

Krank, E. H. 1935. On the crystalline complex of Liverpool Land. Medd. Grønl. 95:1–122.

Krogh, T. E.; Kamo, S. L.; Robinson, P.; Terry, M. P.; and Kwok, K. 2011. U-Pb zircon geochronology of eclogites from the Scandian orogen, northern Western Gneiss Region, Norway: 14–20 million years between eclogite crystallization and return to amphibolite-facies conditions. Can. J. Earth Sci. 48:441–472. doi:10.1139/E10-076.

Kylander-Clark, A. R. C., and Hacker, B. R. 2014. Age and significance of felsic dikes from the UHP Western Gneiss Region. Tectonics 33:2342–2360. doi:10.1002/2014TC003582.

Kylander-Clark, A. R. C.; Hacker, B. R.; and Mattinson, J. M. 2008. Slow exhumation of UHP terranes: titanite and rutile ages of the Western Gneiss Region, Norway. Earth Planet. Sci. Lett. 272:531–540.

Kylander-Clark, A. R. C.; Hacker, B. R.; and Mattinson, C. G. 2012. Size and exhumation rate of ultrahigh-pressure terranes linked to orogenic stage. Earth Planet. Sci. Lett. 321–322:115–120.

Labrousse, L.; Jolivet, L.; Andersen, T. B.; Agard, P.; Hébert, R.; Maluski, H.; and Shärer, U. 2004. Pressure-temperature-time deformation history of the exhumation of ultra-high pressure rocks in the Western Gneiss Region, Norway. Geol. Soc. Am. Spec. Pap. 380: 155–183.

Nakamura, D. 2009. A new formulation of garnet-clinopyroxene geothermometer based on accumulation and statistical analysis of a large experimental data set. J. Metamorph. Geol. 27:495–508.

Nickel, K. G., and Green, D. H. 1985. Empirical geothermobarometry for garnet peridotites and implications for the nature of the lithosphere, kimberlites and diamonds. Earth Planet Sci Lett 73:158–170.

Pedersen, L. E. 2011. Zircon provenance of Devonian deposits in western Norway. MSc thesis, University of Bergen, Bergen.

Powell, R. 1985. Regression diagnostics and robust regression in geothermometer/geobarometer calibration: the garnet-clinopyroxene geothermometer revisited. J. Metamorph. Geol. 2:33–42.

Ravna, E. J. K. 2000. The garnet-clinopyroxene geothermometer—an updated calibration. J. Metamorph. Geol. 18:211–219.

Rehnström, E. F. 2010. Prolonged Paleozoic magmatism in the East Greenland Caledonides: some constraints from U-Pb ages and Hf isotopes. J. Geol. 118: 447–465.

Rex, D. C., and Gledhill, A. R. 1981. Isotopic studies in the East Greenland Caledonides 72°–74°N—Precambrian and Caledonian ages. Rapp. Grøn. Geol. Undersøg. 104:47–72.

Røhr, T. S.; Bingen, B.; Robinson, P.; and Reddy, S. M. 2013. Geochronology of Paleoproterozoic augen gneisses in the Western Gneiss Region, Norway: evidence for Sveconorwegian zircon neocrystallization and Caledonian zircon deformation. J. Geol. 121:105–128.

Root, D. B.; Hacker, B. R.; Gans, P. B.; Ducea, M. N.; Eide, E. A.; and Mosenfelder, J. L. 2005. Discrete ultrahigh-pressure domains in the Western Gneiss Region, Norway: implications for formation and exhumation. J. Metamorph. Geol. 23:45–61.

Sizova, E.; Gerya, T.; and Brown, M. 2012. Exhumation mechanism of melt-bearing ultrahigh pressure crustal rocks during collision of spontaneously moving plates. J. Metamorph. Geol. 30:927–955.

Slama, J., and Pedersen, R. B. 2015. Zircon provenance of SW Caledonian phyllites reveals a distant Timanian sediment source. J. Geol. Soc. 172:465–478. doi:10.1144/jgs2014-143.

Slama, J.; Walderhaug, O.; Fonneland, H.; Kosler, J.; and Pedersen, R. B. 2011. Provenance of Neoproterozoic to upper Cretaceous sedimentary rocks, eastern Greenland: implications for recognizing the sources of sediments in the Norwegian Sea. Sediment. Geol. 238: 254–267. doi:10.1016/j.sedgeo.2011.04.018.

Taylor, W. R. 1998. An experimental test of some geothermometer and geobarometer formulations for upper mantle peridotites with application to the thermobarometry of fertile lherzolite and garnet websterite. N. Jb. Mineral. Abh. 172:381–408.

Templeton, J. A. 2015. Structural evolution of the Hornelen Basin (Devonian, Norway) from detrital thermochronology. PhD dissertation, Columbia University, New York.

Thrane, K. 2002. Relationships between Archean and Paleoproterozoic crystalline basement complexes in the southern part of the East Greenland Caledonides: an ion microprobe study. Precambrian Res. 113:19–42.

Torsvik, T. H.; Van der Voo, R.; Preeden, U.; Niocaill, C. M.; Steinberger, B.; Doubrovine, P. V.; van Hinsbergen, D. J. J.; et al. 2013. Phanerozoic polar wander, paleogeography and dynamics. Earth Sci. Rev. 114:325–368. doi:10.1016/j.earscirev.2012.06.007.

Tucker, R. D.; Krogh, T. E.; and Råheim, A. 1992. Proterozoic evolution and age-province boundaries in the central part of the Western Gneiss Region, Norway: results of U-Pb dating of accessory minerals from Trondheimsfjord to Geiranger. Geol. Assoc. Can. Spec. Pap. 38:149–173.

White, A. P., and Hodges, K. V. 2002. Multistage extensional evolution of the central East Greenland Caledonides. Tectonics 21. doi:10.1029/2001TC001308.

Yin, A.; Manning, C. E.; Lovera, O. M.; Menold, C.; Chen, X.; and Gehrels, G. 2007. Early Paleozoic tectonic and thermomechanical evolution of ultrahigh-pressure (UHP) metamorphic rocks in the northern Tibetan Plateau, northwest China. Int. Geol. Rev. 49:681–716.